TABLE OF CONTENTS

Page

CHAPTER 8. SEDIMENTATION AND EROSION HYDRAULICS 8-1

8.1 INTRODUCTION...8-1

8.2 PROPERTIES OF SEDIMENT 8-3

8.2.1 Particle Size... 8-3
8.2.2 Particle Shape 8-4
8.2.3 Specific Gravity of Particles 8-5
8.2.4 Fall Velocity 8-5
8.2.5 Sediment Size Distribution and Gradation Curves 8-5

8.3 SEDIMENT LOAD IN ALLUVIAL CHANNELS...8-6

8.3.1 Sediment Transport Analysis 8-8
8.3.2 Suspended Load 8-8
8.3.3 Bed Load 8-11
8.3.4 Transition Between Bed Load and Suspended Load 8-14
8.3.5 Total Bed Material Sediment Load.. 8-14

8.4 RESISTANCE TO FLOW 8-15

8.4.1 Common Resistance Parameters and Sediment Characteristics 8-15
8.4.2 Bed Forms.. 8-16
8.4.3 Boundary Shear Stress Calculations 8-17
8.4.4 Incipient Motion Analysis 8-19

8.5 SEDIMENT TRANSPORT EQUATIONS..8-21

8.5.1 Meyer-Peter and Muller Equation 8-23
8.5.2 Empirical Power Relationships 8-23
8.5.3 Colby's Approach 8-29
8.5.4 Modified Einstein Method.. 8-33
8.5.5 Unit Stream Power Method... 8-33

LIST OF FIGURES

Figure 8-1. Example of Sediment Degradation in Calabazas Creek 8-2
Figure 8-2. Example of Channel Downgrading in Stevens Creek 8-2
Figure 8-3. Example of Bank Erosion in Thompson Creek 8-3
Figure 8-4. AGU Standard Sediment Gradation Graph Paper 8-6
Figure 8-5a. Definition of Sediment Load Components (Simons, Li & Associates, Inc., [1982]) 8-7
Figure 8-5b. Definition Sketch of Suspended Sediment Concentration Distributions 8-9
Figure 8-5c. Factor x in the Velocity Distribution Equation 8-10
Figure 8-6a. Eistein's Bed Load Transport Relationship [Einstein 1950]............................... 8-12
Figure 8-6b. Factor ξ in Eistein's Bed Load Function in Terms of d_{si}/X................................ 8-13

Page

Figure 8-6c. Factor Y_c in Einstein's Bed Load Function in Terms of d_{65}/δ 8-14
Figure 8-7. Bed Forms as a Function of Stream Power and Fall Diameters of Bed Sediment [Simons and Richardson 1966] 8-17
Figure 8-8. Distribution of Boundary Shear Stress 8-18
Figure 8-9. Maximum Unit Tractive Force for Various Channel Geometries, Lane and Carlson [1953] 8-19
Figure 8-10. Effect of Curvature on Boundary Shear Stress 8-20
Figure 8-11a. Shields Diagram With Additional Data From Several Other Researchers 8-20
Figure 8-11b. Adjusted Shields Diagram Per Gessler [1971] 8-21
Figure 8-12. Colby [1964] Bed Load Transport Relationships 8-30
Figure 8-13. Water Temperature Correction Factor 8-31
Figure 8-14. Fine Sediment Correction Factor 8-31
Figure 8-15. Correction for Median Particle Size 8-32

LIST OF TABLES

Table 8-1 Sediment Grade Scale 8-4
Table 8-2 Summary of Some Commonly Used Sediment Transport Equations 8-22
Table 8-3 Results of Regression Analysis for Empirical Power Relationships ($q_{bmT} = a Y_h^b V^c$) when $0.001 \le S_o \le 0.01$ 8-25
Table 8-4 Results of Regression Analysis for Empirical Power Relationships ($q_{bmT} = a Y_h^b V^c$) when $0.01 \le S_o \le 0.04$ 8-26
Table 8-5 Range of Parameters Examined for Power Relationship 8-29

BIBLIOGRAPHY

CHAPTER 8. SEDIMENTATION AND EROSION HYDRAULICS

8.1 INTRODUCTION

When water flows, it has the ability to mobilize sand, gravel, or even large boulders from the bed or banks, and deposit them at downstream locations. This natural process is called sediment transport, and the analysis to examine the sediment transport phenomena is called sediment transport analysis.

Sediment transport is one of the major contributors to the shaping of landforms. Human has tried to understand and control this process for thousands of years. Due to the complexity of this process, many features of sediment transport are still imperfectly understood. However, progress continues to be made on the subject by many researchers and engineers.

A variety of terminology has been used to describe channel response to changing sediment transport conditions. The following definitions are adopted in this manual to avoid confusion.

Aggradation and degradation are the raising or lowering of channel bed, respectively, occurring over relatively long reaches from changes such as sediment supply, rainfall and runoff patterns, and man-induced effects. General scour/deposition refers to more localized vertical changes of the channel bed, for example, the general scour/deposition in a given reach after passage of a single flood. Local scour is caused by vortices resulting from local disturbances in the flow such as bridge piers and embankments. In general, the vertical changes in a channel are additive so that, for example, local scour could be occurring in a reach experiencing general scour and/or aggradation.

Lateral migration is defined as bank alignment shifting due to bank erosion. Since aggradation/degradation, general scour/deposition, and/or any local scour along an embankment could promote bank instability, the vertical and horizontal shifting on a channel is interrelated.   Degradation, general scour, local scour and lateral migration could endanger adjacent property, bridge and other hydraulic structures, while aggradation and deposition could reduce channel capacity, increase lateral erosion and increase flooding potential.

In most watershed-management projects, sediment transport plays an important role for the success of the project. The sediment data, along with other creek characteristics such as channel slope, cross-sectional geometry and roughness factors, will determine the creek's stability. Without proper sediment transport analysis, the project may fail to understand the creek's tendency to change, and cause channel modification work to fail. Figure 8-1 shows a photograph of the Calabazas Creek downstream of Pruneridge Avenue. Five feet of bed degradation occurred in 6 years. It appears that the creek's capacity for degradation far exceeded engineers' calculation.

Figure 8-1. Example of Sediment Degradation in Calabazas Creek

Another example of channel degradation is shown in Figure 8-2 for Stevens Creek at Dana Avenue. Although vegetation protects the banks, the channel bottom is being eroded. Evidence of the armoring process (see Section 2.3.5) is shown near the foreground.

Figure 8-2. Example of Channel Downgrading in Stevens Creek

Figure 8-3 below shows the bank erosion occurring at Thompson Creek downstream of Aborn Road. Without vegetative protection, the outer bank of a mild bend has been eroded to a vertical wall, with evidence of continuous toe failure.

Figure 8-3. Example of Bank Erosion in Thompson Creek

These pictures illustrate the types of sedimentation problems we have. Below is a description of sediment properties that affect the particles' movement in water, before the hydraulics of sediment transport is presented.

8.2 PROPERTIES OF SEDIMENT

The sedimentation process depends not only on the characteristics of the flow involved, but also on the properties of the sediment itself. Those properties of most importance include the size of the sediment particle or grain, the specific weight, shape, and settling velocity. Flocculation may be of importance in the behavior of fine sediments. These properties will be described briefly in the following.

8.2.1 Particle Size

Because the size and shape of a sediment particle vary over wide ranges, it is often necessary to determine averages or statistical values, and it is convenient to group sediments into different size classes or grades. For size classifications, a system proposed by the subcommittee on Sediment Terminology of the American Geophysical Union and ASCE is shown in Table 8-1. It has the advantage of sizes being arranged in a geometric series with a ratio of two. It also has sizes corresponding closely to the mesh opening in sieves in common use.

Note that the smallest sieve has a mesh size of 1/16 of a millimeter, which by definition is the size dividing the sands and silts. It also corresponds roughly to the finest sediment found in appreciable quantities in the beds of most streams.

Table 8-1
Sediment Grade Scale

Class Name	Size Range			Approximate Sieve Mesh Openings per inch
	Millimeters		Inches	
Very large boulders		4096 – 2048	160 – 80	
Large boulders		2048 – 1024	80 – 40	
Medium boulders		1024 – 512	40 – 20	
Small boulders		512 - 256	20 – 10	
Large cobbles		256 – 128	10 – 5	
Small cobbles		128 – 64	5 – 2.5	
Very coarse gravel		64 – 32	2.5 – 1.3	
Coarse gravel		32 – 16	1.3 – 0.6	
Medium gravel		16 – 8	0.6 – 0.3	
Fine gravel		8 – 4	0.3 – 0.16	5
Very fine gravel		4 - 2	0.16 – 0.08	10
Very coarse sand	2 - 1	2 – 1		18
Coarse sand	1 – 1/2	1 – 0.5		35
Medium sand	½ - 1/4	0.5 – 0.25		60
Find sand	¼ - 1/8	0.25 – 0.125		120
Very fine sand	1/8 – 1/16	0.125 – 0.062		230
Coarse silt	1/16 – 1/32	0.062 – 0.031		
Medium silt	1/32 – 1/64	0.031 – 0.016		
Fine silt	1/64 – 1/128	0.016 – 0.008		
Very fine silt	1/128 – 1/256	0.008 – 0.004		
Coarse clay	1/256 – 1/512	0.004 – 0.002		
Medium clay	1/512 – 1/1024	0.002 – 0.001		
Fine clay	1/1024 – 1/2048	0.001 – 0.0005		
Very fine clay	1/2048 – 1/4096	0.0005– .00024		

Since natural sediment particles are of irregular shape, we need to choose a method of measurement to define the particle size. Two methods are commonly used. One is the Sieve Diameter which is the length of the side of a square sieve opening through which the given particle will just pass. The other is the Sedimentation Diameter which is the diameter of a sphere of the same specific weight and terminal settling velocity as the given particle in the same sedimentation fluid. The size of sands is commonly measured by the former (sieving), and the size of silts and clays is generally expressed as the latter and determined by sedimentation methods because of convenience. The sedimentation methods include the pipet method, bottom withdrawal method, and the hydrometer method. These methods are discussed in [ASCE 1975].

8.2.2 Particle Shape

Particle shape is usually determined by the shape factor, SF.

$$SF = \frac{c}{\sqrt{ab}}$$

where a, b, and c are the lengths of the longest axis, the intermediate axis, and the shortest axis, respectively. These axes are mutually perpendicular. A sphere would have a shape factor of 1. Natural sediment typically has a shape factor of 0.7. Particle shape affects the fall velocity, and hence, the sedimentation process.

8.2.3 Specific Gravity of Particles

In natural soils, the specific gravity ranges from 2.6 to 2.8, with the lower values corresponding to coarse soils and higher values for fine-grained soil type. Due to its resistance to weathering and abrasion, quartz, which has a specific gravity of 2.65, is the most common mineral found in natural non-cohesive sediment. Therefore, in sedimentation studies, it is customary to assume 2.65 as the particle specific gravity. However, for our projects, the actual specific gravity for the site material should always be measured.

8.2.4 Fall Velocity

After a particle is set in motion in the stream, through mechanisms of shear and lift forces and turbulence, it tends to settle back to the bed by gravity. Fall velocity is a general term describing the rate of fall or settling of a particle. It is the most fundamental property governing the motion of a sediment particle. It is a function of the volume, shape and density of the particle and the viscosity and density of the fluid. It is used in many sediment transport equations, e.g., Einstein [1950], Laursen [1958], Toffaletti [1969], etc. ASCE [1975] provides equations and charts to determine fall velocity based on particle size, shape factor, water temperature and sediment concentration.

8.2.5 Sediment Size Distribution and Gradation Curves

The variation in particle sizes in a sediment mixture is described with a gradation curve, which is a cumulative size-frequency distribution curve showing particle size versus accumulated percent finer, by weight. It is common to refer to particle sizes according to their position on the gradation curve. For example, d_{50} is the mean particle size, i.e., 50 percent of the sample is finer by weight; $d_{84.1}$ is 1 standard deviation larger than the mean size; and $d_{15.9}$ is 1 standard deviation smaller than the mean size. Geometric mean particle size d_g and geometric deviation σ_g are also used in the literature to describe particle size distributions:

$$d_g = \sqrt{d_{84} d_{16}}$$

$$\sigma_g = \sqrt{d_{84} / d_{16}}$$

Note that these definitions for the geometric mean and standard deviation assume that the sizes are logarithmically distributed, i.e., the logarithms of the grain sizes are normally distributed, which is usually true. However, the common practice has been to use these definitions even if the distribution is not logarithmic. The sediment size distribution is typically described by a cumulative size-frequency curve. This is presented on log-normal graph paper as grain-size vs. percent finer, as shown in Figure 8-4. The grain size on the abscissa is the standard sediment classification adopted by the American Geophysical Union (AGU) and listed in Table 8-1. Natural sediment samples typically appear in a reversed S shape in this plot.

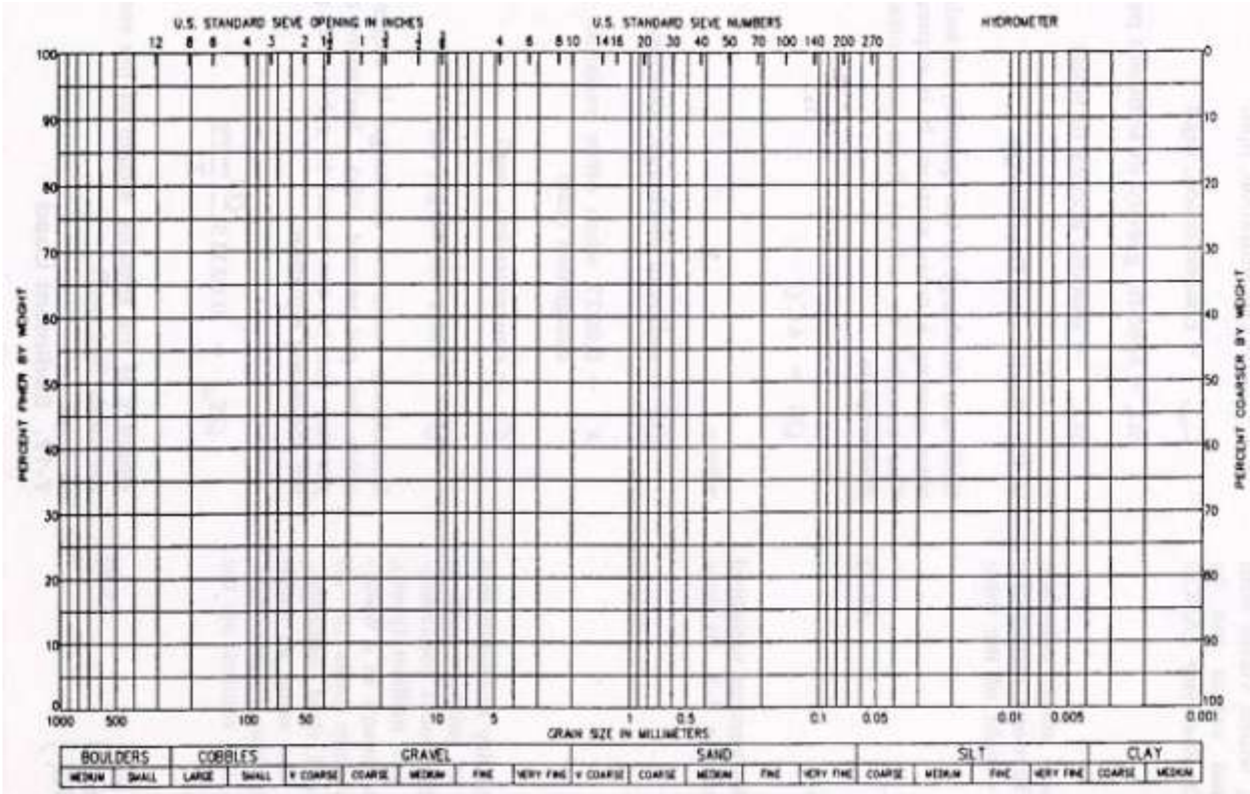

Figure 8-4. AGU Standard Sediment Gradation Graph Paper

8.3 SEDIMENT LOAD IN ALLUVIAL CHANNELS

The sediment load in alluvial channels may be classified into *wash load* and *bed-material load*. The wash load is defined as the relatively fine sediment transported in alluvial channels that does not contribute to the bed material composition significantly. The bed-material load, on the other hand, is the sediment transported in alluvial channels that constitutes significant amounts of the channel bed. In other word, most of the wash load is transported through the system and little is deposited on or in the channel bed.

Figure 8-5a presents the definition of all the sediment load components. Some engineers assume that the size of bed-material particles is equal to or larger than 0.0625 mm, which is the dividing point between sand and silt. The sediment load consisting of grains smaller than this size is considered wash load. Another approach, as adopted by Einstein [1950], is to choose a sediment size finer than ten percent of the bed sample as the dividing size between wash load and bed-material load.

The presence of wash load can increase bank stability, reduce seepage and increase bed-material transport. Wash load can be easily transported in large quantities by the water flows, and is usually limited by availability from the watershed. The magnitude of wash load is dependent on the upstream supply of the source and cannot be calculated based on sediment transport relationships and bed material composition. That is why most of the published sediment transport formulas only deal with the bed-material load.

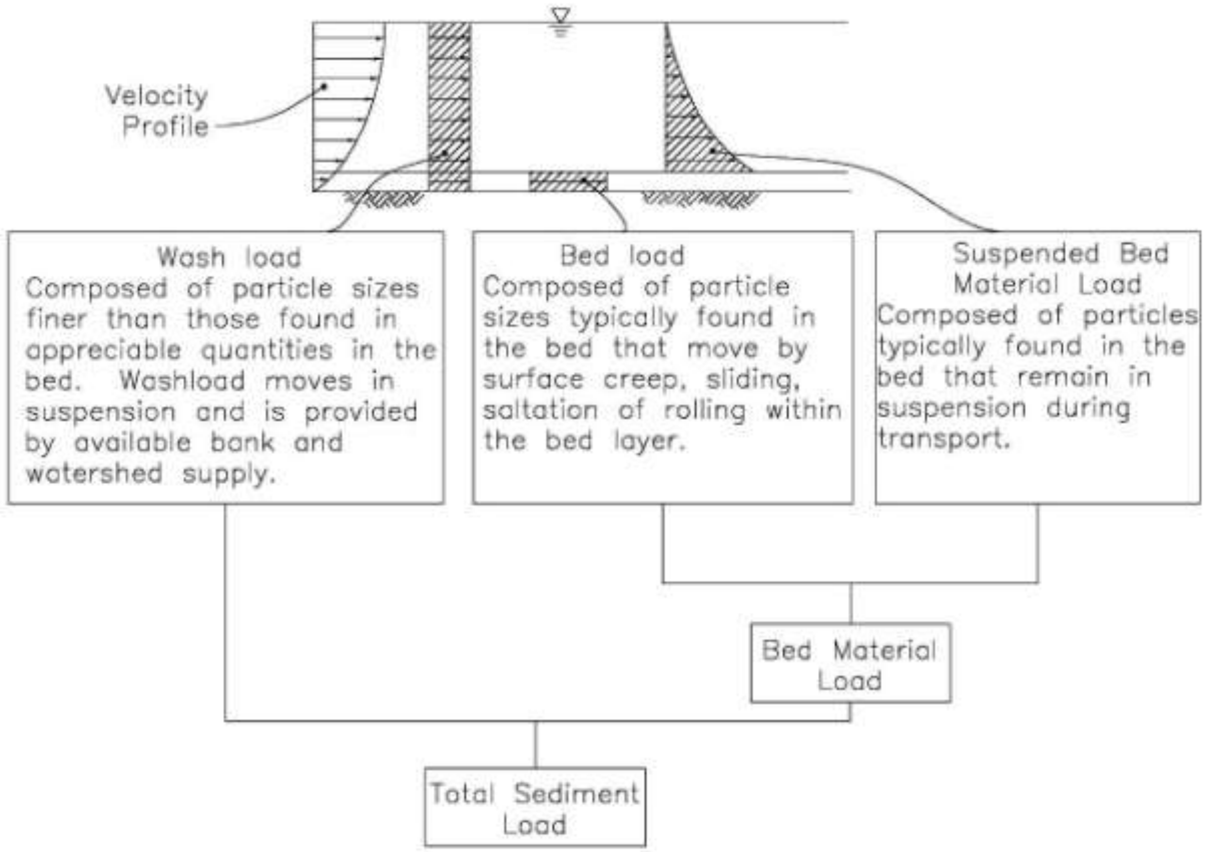

Figure 8-5a. Definition of Sediment Load Components (Simons, Li & Associates, Inc., [1982])

There are three ways in transporting sediment particles in alluvial channels, namely surface creep, saltation, and suspension. *Surface creep* is the rolling or sliding of particles along the bed. *Saltation* (jumping) is the cycle of motion above the bed with resting periods on the bed. *Suspension* is when sediment particles are suspended in the water column through the motion of transportation.

In the Einstein sediment transport relationship [Einstein 1950], the bed-material load is further divided into bed load and suspended load. According to Einstein [1950], bed load is defined as the portion of sediment load with particles moving in the bed layer in motions of rolling, sliding and saltation; and suspended load is the portion of sediment load with particles moving above the bed layer. The bed layer is defined as a flow layer, **2-grain-diameter thick**, immediately above the bed. The thickness of the bed layer varies with the particle size. The suspended load consists of sands, silts, and clays.

Total sediment load is defined as the sum of bed load and suspended load, or the sum of bed-material load and wash load. The calculations described in the next sections for suspended and bed loads only address the bed-material load.

At low transport rates or in shallow flow, the bed load may approximate the total load. Conversely, in a deep river or at high flow rates, the bed load may only account for 5-10% of the total load. The Upper Guadalupe Creek [PWA, 1996] used a value of 10 percent, and the measured bed load in Berryessa Creek [USACE, 2004] was about 15% of suspended load. Our measured data in Calabazas Creek at 80 cfs show a bed load of approximately 10% of the total load. Although the amount of bed load may be small compared to total sediment load, it is important because it shapes the bed form and influences channel stability and bed roughness.

8.3.1 Sediment Transport Analysis

In general, there are 3 approaches to examine the transport of sediment in turbulent flow. The oldest was the approach of Shields [1936] and DuBoys [Brown 1950] relating sediment discharge to excess bottom shear stress. When the shear stress on the stream bed exceeds a critical value for a particle size and density, the sediment may be moved by the flow and result in transport. Since these relationships involve only the excess bottom-shear-stress, it is reasonable to expect that they apply only to bed load transport.

The second approach is that of Einstein [1950] incorporating both probability and fluid mechanics in formulating sediment transport equations. Einstein argued that the movement of a particle from the bed depended on the probability of the lift force on the particle being greater than the settling force. Since the natural flow is turbulent in most cases, this concept of linking probability to bed load movement is logical. Einstein also integrated the product of flow velocity with sediment concentration over the water column above the bed layer to estimate the suspended sediment discharge. The bed load and suspended load are summed up to compute the total sediment discharge. Einstein's expression for sediment discharge includes parameters of hydraulic radius, water depth, energy slope, velocity, densities of water and sediment, sediment size, fall velocity and gravity. It is the most complete in terms of inclusion of pertinent variables.

The third approach is the concept of stream power utilized by Bagnold [1966], Ackers and White [1973], Yang [1984], and several other researchers. They hypothesized that the rate of sediment transport should be related to the rate of energy dissipation of, or work done by, the flow. Since work may be expressed as a force exerted over a distance over time, Bagnold used the product of shear stress and flow velocity to represent stream power per unit bed area. Yang used the product of velocity and energy slope to represent stream power per unit weight of water. The stream power may also be expressed in terms of turbulent energy dissipation. Since turbulent energy dissipation is a continuous process applicable to the entire flow domain, it is reasonable to expect this relationship to apply to both suspended and bed loads.

More details of the mechanics of sediment transport are provided below.

8.3.2 Suspended Load

The finer particles of the sediment load of a stream move predominantly as suspended load. The characteristic of a suspended particle is that buoyancy and turbulence of the fluid keep the particle afloat during its entire motion. Based on continuity of mass and using the Prandtl-von Karman velocity defect law to define the velocity distribution in a water column, Hunter Rouse [1937] developed an equation to describe the suspended sediment concentration distribution as follows

$$\frac{C_y}{C_a} = \left(\frac{Y-y}{y}\frac{a}{Y-a}\right)^z \qquad (8\text{-}1)$$

where

$$z = \frac{w}{kV_*} \quad (8\text{-}2)$$

Y is the flow depth, y is the vertical distance above the bed, a is the thickness of the bed layer which is 2 grain diameters thick as assumed by Einstein [1950], C_y and C_a are the suspended sediment concentrtions in dry weight per unit volume at y and a, respectively, above the bed, w is the fall velocity of the sediment, V_* is the shear velocity, and k is von Karman universal constant (0.4). The notations are shown in Figure 8-5b. Equation (8-1) is often referred to in the literature as the Rouse equation.

Since multiplying the suspended sediment concentration with flow velocity and integrating over the water column will generate the suspended sediment discharge per unit width, many researchers have used the Rouse equation in combination with a velocity distribution to develop suspended-sediment transport theories. One most recognized example is the Eistein sediment discharge theory. Einstein's theory links together the supended load and bed load to produce the bed-material load. This theory examines one size fraction of the bed material at a time, and denotes that grain size as d_{si} where d_s stands for the sediment diameter and the subscript *i* stands for the ith size fraction. The theory is summarized in the following paragraphs.

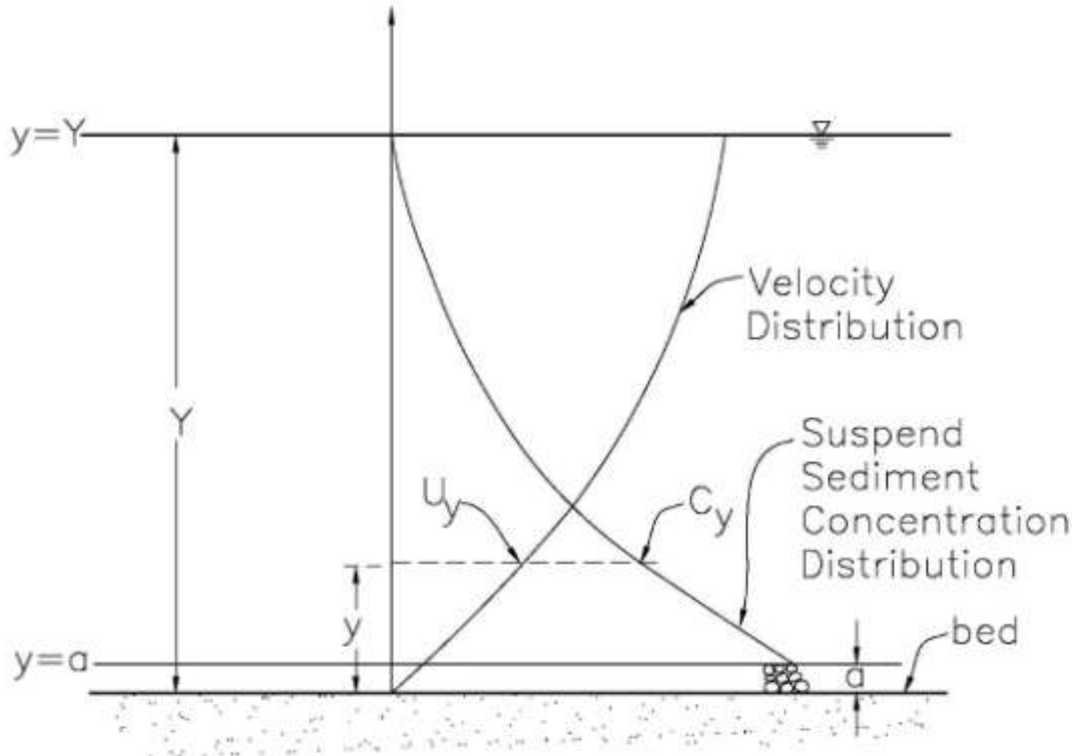

Figure 8-5b. Definition Sketch of Suspended Sediment Concentration Distributions

Einstein [1950] used the velocity distribution proposed by Keulegan [1938]

$$\frac{V_y}{V_*'} = 5.75 \log_{10}(30.2\frac{y}{\Delta}) \quad (8\text{-}3)$$

where V_y is the point velocity at a distance y above the bed, $V_*^{'}$ is the shear velocity based on shear stress due to the grain roughness, and Δ is the apparent roughness of the surface defined as k_s/x where k_s is the equivalent sand grain roughness diameter which may be taken as d_{65} and x is the demensionless factor to account for viscous effect and is determined from Figure 8-5c. See Section 8.4.3 for more discussions on $V_*^{'}$. In Figure 8-5c, the abscisa is k_s/δ, where δ is the thickness of the viscous sublayer and may be estimated by

$$\delta = 11.6 \frac{\nu}{V_*^{'}} \qquad \text{and} \qquad V_*^{'} = \sqrt{g R^{'} S}$$

where ν is the kinematic viscosity, and R' is the hydraulic radius based on grain roughness and may be computed, as recommended by Einstein and Barbarossa [1952], by the Manning-Strickler equation:

$$\frac{V}{\sqrt{g R^{'} S}} = 7.66 \left(\frac{R^{'}}{k_s}\right)^{1/6}$$

x

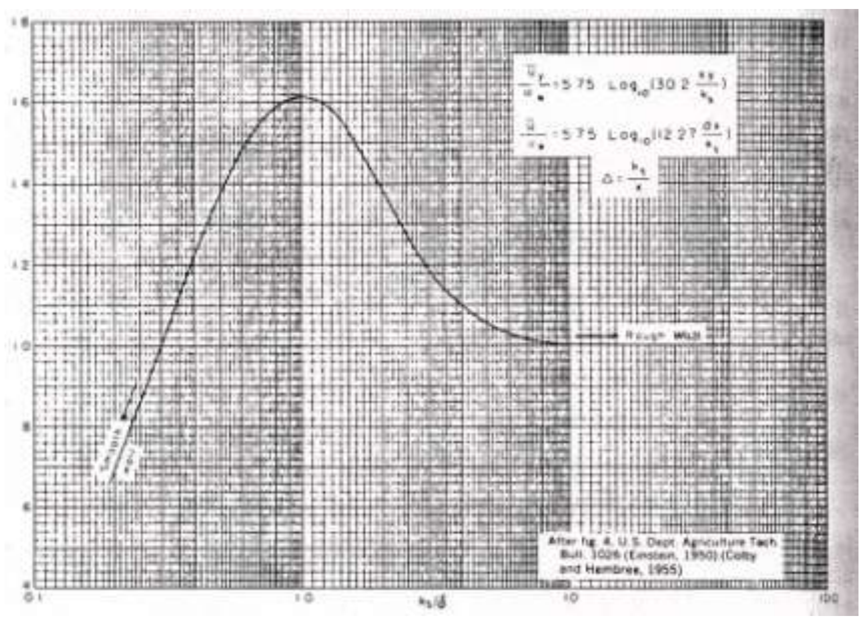

Figure 8-5c. Factor x in the Velocity Distribution Equation

The suspended load per unit width is the integral, of the product of point velocity and suspended sediment concentration, from the top of the bed layer ($y = a = 2d_{si}$) to the water surface ($y = Y$). This is mathematically expressed as follows

$$\begin{aligned} q_{si} &= \int_a^Y C_y V_y \, dy \\ &= \int_a^Y C_a \left(\frac{Y-y}{y} \frac{a}{Y-a} \right)^z V_*^{'} 5.75 \log_{10} \left(30.2 \frac{y}{\Delta} \right) dy \end{aligned} \qquad (8\text{-}4)$$

where q_{si} is the suspended sediment discharge per unit width for the ith fraction. After transformation of variables, Einstein presented Equation 8-4 in the following form:

$$q_{si} = 11.6 V_*^{'} C_a a \left[2.3 \log_{10}\left(30.2 \frac{Y}{\Delta} \right) I_1 + I_2 \right] \quad (8\text{-}5)$$

with

$$I_1 = 0.216 \frac{A^{z-1}}{(1-A)^z} \int_A^1 \left(\frac{1-y'}{y'}\right)^z dy' \quad (8\text{-}6a)$$

$$I_2 = 0.216 \frac{A^{z-1}}{(1-A)^z} \int_A^1 \left(\frac{1-y'}{y'}\right)^z \log_e(y')\, dy' \quad (8\text{-}6b)$$

In Equations. (8-6a) and (8-6b), y' = y/Y and A = a/Y = $2d_{si}$/Y. Note that z = w/(kV_*') here, different from that of the Rouse Equation in Eq. (8-2). Equations (8-5) and (8-6) are evaluated for each size fraction.

8.3.3 Bed Load

Einstein assumed that the bed-load layer for each size fraction is 2-grain-diameter ($2d_{si}$) thick. Within this small depth, the velocity and sediment concentration were assumed constant. Hence the bed load discharge may be written as

$$q_{bi} = \alpha C_{ai} (2 d_{si}) V_b$$

where q_{bi} is the bed-load discharge of the ith fraction per unit width and V_b is the flow velocity at the bed and α is a coefficient. Einstein approximated the bed velocity with the shear velocity and used experimental data to calibrate this equation and developed the following formula:

$$q_{bi} = 11.6 C_{ai} 2 d_{si} V_*^{'} \quad (8\text{-}7)$$

Since this formula still depends on the unknown sediment concentration of the bed layer, C_{ai}, Einstein [1950] developed his Bed Load Function to bridge the gap. The bed load function defines the relationship between ψ_* and ϕ_*, as shown graphically in Figure 8-6a.

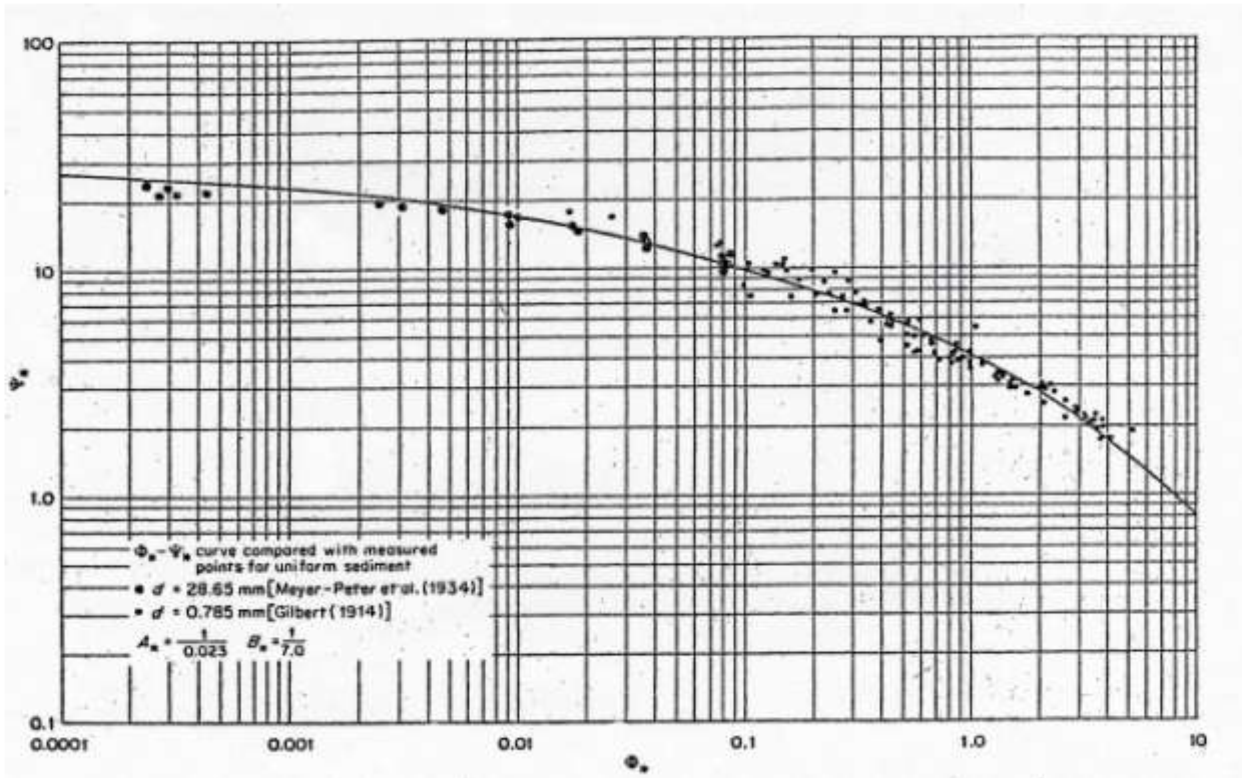

Figure 8-6a. Eistein's Bed Load Transport Relationship [Einstein 1950]

The parameter ϕ_{*i}, called "intensity of transport" for individual grain size, is defined as follows

$$\phi_{*i} = \frac{q_{bi}}{i_b \rho_s g} \left(\frac{\rho_f}{\rho_s - \rho_f} \right)^{1/2} \left(\frac{1}{g d_{si}} \right)^{1/2} \tag{8-8}$$

where q_{bi} is the bed load per unit width for a bed-material size d_{si}, i_b is the weight fraction of this bed material of size d_{si}, ρ_s and ρ_f are, respectively, the densities of bed particles and fluid, and g is the gravity acceleration. The parameter, ψ_{*i}, called "Intensity of Shear" for an individul grain size, is the inverse of the dimensionless bottom shear stress and defined as follows

$$\psi_{*i} = \xi Y_c \left(\frac{\beta}{\beta_*} \right)^2 \frac{\rho_s - \rho_f}{\rho_f} \frac{d_{si}}{R_b' S} \tag{8-9}$$

where ξ is the hiding factor of grains in a mixture and may be determined from Figure 8-6b, Y_c is the presure correction factor for boundary roughness and may be determined from Figure 8-6c, $\frac{\beta^2}{\beta_*^2}$ is a factor accounting for the effect of grain mixture and is defined below, S is the channel slope, and R_b' is the hydraulic rdius of the channel bed due to grain roughness.

$$\beta = \log 10.6 \qquad \text{and} \qquad \beta_* = \log \frac{10.6 x X}{d_{65}} \tag{8-10}$$

where $$X = 0.77\frac{d_{65}}{x} \text{ when } \frac{d_{65}}{x\delta} > 1.80$$

and $$X = 1.398\delta \text{ when } \frac{d_{65}}{x\delta} < 1.80$$

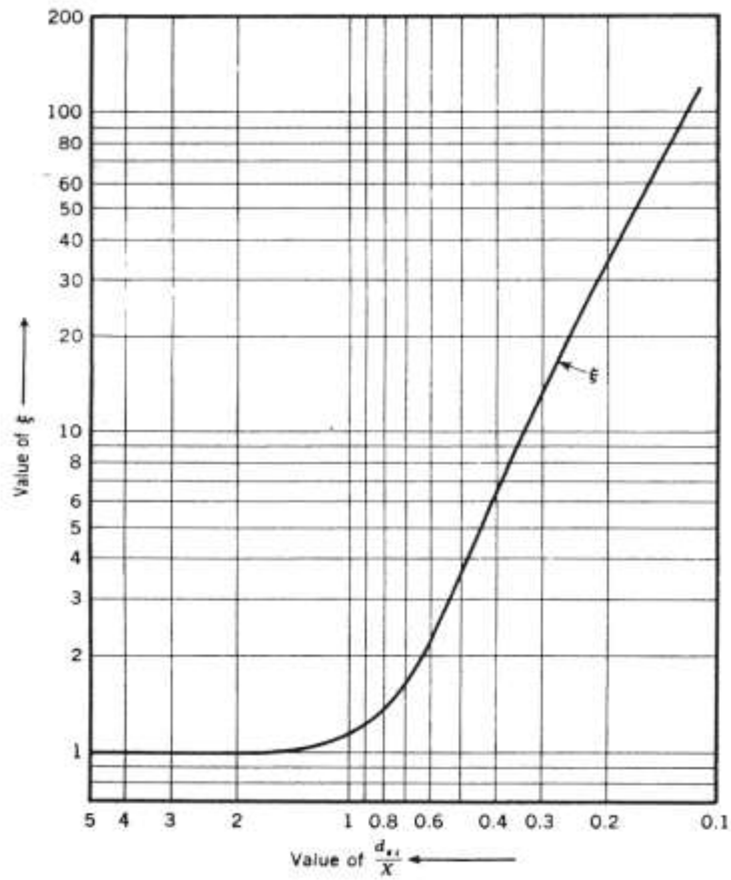

Figure 8-6b. Factor ξ in Eistein's Bed Load Function in Terms of d_{si}/X

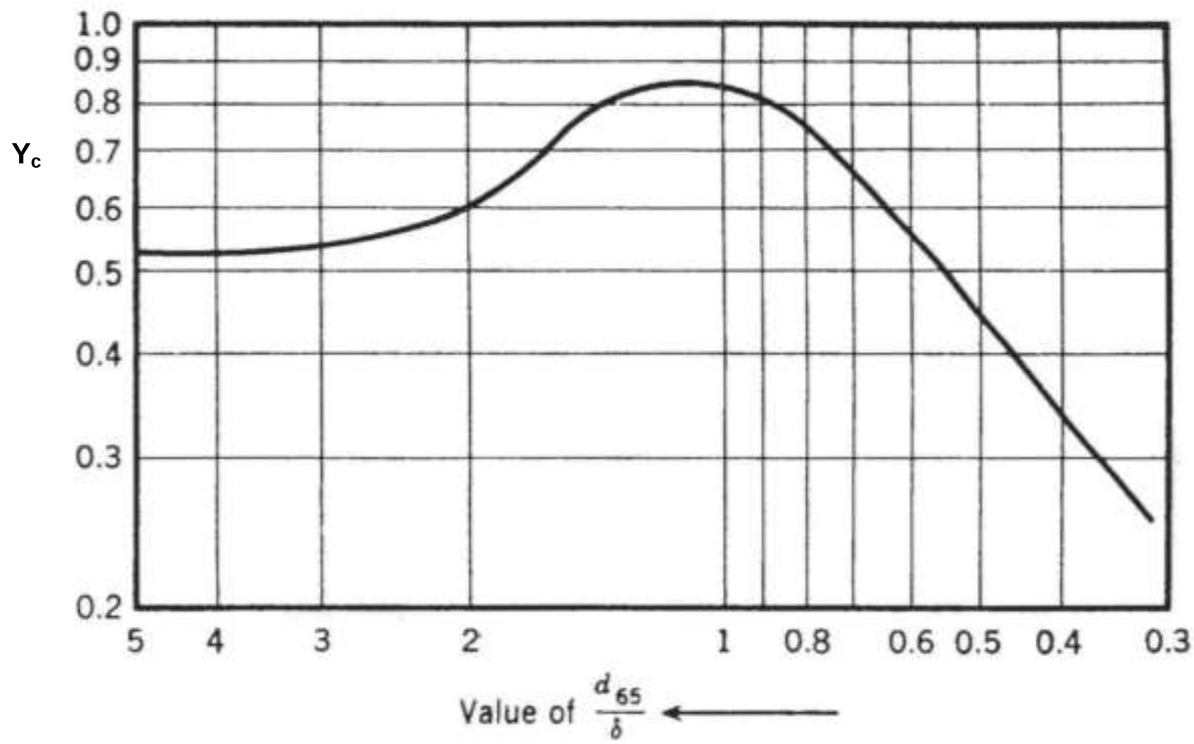

Figure 8-6c. Factor Y_c in Einstein's Bed Load Function in Terms of d_{65}/δ

Calculation of the sediment discharge using the Einstein bed load function is carried out in three parts. First, collect field data of slope, cross-sectional geometry, and bed material. Determine weight fractions of several grain sizes d_{si} along with the specific density ρ_s, d_{35} and d_{65}. Estimate friction factor of channel banks. Secondly, determine the bed hydraulic radius due to grain roughness, R_b', for a number of discharges. Thirdly, determine ψ_{*i}, determine ϕ_{*i} using the graphicaal relationship in Figure 8-6a, and compute bed load q_{bi} for a given grain size d_{si}. The summation of all q_{bi} will be the bed load q_b.

8.3.4 Transition Between Bed Load and Suspended Load

When the bed load, q_{bi}, for each fractional size of bed material is determined, Equation 8-7 is used to compute the sediment concentration of this size of material, C_{ai}, in the bed layer. The assumption, as proposed by Einstein [1950], is that the point suspended sediment concentration C_{ai} can be taken as the average concentration of that material in the bed layer. After C_{ai} has been calculated, the suspended load for the given grain size, q_{si}, is computed using Equation 8-5.

8.3.5 Total Bed Material Sediment Load

The total bed material sediment load for a given grain size is the sum of the bed load and suspended load. Let q_{bmTi} denotes the total bed-material load per unit width for fractional size d_{si}. It can be expressed as follows

$$
\begin{aligned}
q_{bmTi} &= q_{si} + q_{bi} \\
&= 11.6 V_*^{'} C_a a \left[2.3 \log_{10}\left(30.2\frac{Y}{\Delta}\right) I_1 + I_2 \right] + 11.6 C_a V_*^{'} a \\
&= q_{bi}\left(1 + P I_1 + I_2\right)
\end{aligned}
$$

where

$$P = \frac{1}{0.434}\log_{10}\left(\frac{30.2Y}{\Delta}\right) \tag{8-12}$$

The same procedure is performed to calaulate the sediment load for each size fraction of the bed material. The sum of all sediment loads for all size fractions is the total bed-material load per unit width of the channel. Multiplying this value by the channel width, the total bed mterial load over the entire channel cross-section is obtained.

8.4 RESISTANCE TO FLOW

Section 7.6 in Chapter 7 has discussed the basic formulae of flow resistance, namely the concept of bottom shear stress, τ_o, and the Darcy-Weisbach, Chezy and Manning's equations. Those relationships apply to channels of a flat bottom surface, which may not always exist when sediment is present. In the following further discussions will be made to address channel roughness in light of sediment transport analysis.

8.4.1 Common Resistance Parameters and Sediment Characteristics

Several empirical formulae have been suggested that relate the bed-material size to Manning's friction coefficient, n. For sand-bed channels, Meyer-Peter and Muller [1948] recommend

$$n = \frac{d_{90}^{1/6}}{26} \tag{8-13}$$

where D_{90} is the particle size in **meters** for which 90% of the sediment by weight is finer. Note that if the unit of d_{90} is converted to feet, this formula is the same as Eq. (7-24), if the d in Eq. (7-24) is taken as d_{90}. As pointed out by Henderson [1966], the effective value of d from the resistance viewpoint, is that of the larger size, two or three times the median d_{50}, with which the bed tends to become armored. For the size distributions of bed materials of most of our creeks, this indicates that d_{80} or d_{90} should be used to in Eq. (7-24). Strickler's [1923] orginal derivation based on gravel-bed streams showed

$$n = 0.034 d_{50}^{1/6}$$

where d_{50} is expressed in **feet**. This relationship compares well to Eq. (8-13) or Eq. (7-24) when d_{90} is used. The Corps of Engineers' experiments [Maynord 1991] showed that the Strickler equation will give satisfactory n-values using d_{90}.

Based on their San Luis Valley Study where the beds of the canals were covered with cobbles, Lane and Carlson [1953] suggested the following formula

$$n = \frac{d_{75}^{1/6}}{39} \tag{8-14}$$

where D_{75} is the particle size in **inches** for which 75% by weight of sediment is finer. After converting the unit to feet and changing d75 to d90, this equation also falls in the same range as Eq. (8-13).

In a Highway Research Board publication, Anderson et al. [1970] recommend

$$n = 0.0395 d_{50}^{1/6} \tag{2-15}$$

where D_{50} is 50% finer particle size in **feet**. Note that this produces a friction coefficient 15% higher than that given by Strickler's equation.

8.4.2 Bed Forms

The Manning's friction coefficient presented in Eqs. (8-13) to (8-15) were derived for flat-channel-bed conditions. In these cases, the resistance force is mainly generated by skin friction on the surface of the bed and bank materials. This friction coefficient will increase when the bed form takes on other more complex configurations. In natural sand-bed channels, the bed has been observed to be flat or undulating in forms of ripples, dunes or antidunes, depending on the discharge and water depth. These ripples, dunes and antidunes generate additional form drag to the grain roughness of the flat bed. A detail discussion of bed forms and their characteristics is provided by Simons and Senturk [1977] and Simons, Li & Associates, Inc. [1982]

Figure 8-7 presents the bed form as a function of median fall diameter and stream power. Median fall diameter may be approximated by the median diameter (d_{50}), which is known from bed-material gradation analysis. The stream power is defined as the product of velocity (V) and boundary shear stress (τ_0), it is a function of hydraulic conditions as determined by the water-surface profile calculations.

As shown in Figure 8-7, these complex bed forms occur in channels of median sediment sizes less than 1 mm. Within the Santa Clara Valley, due to our relative proximity between the upper watersheds and the Bay, sediments in our creeks are usually much coarser than this size. Typically our d_{50} is in the order of 10 mm. Hence, these bed forms, other than flat bed, are rarely seen in our area. The riffles and pools that we observe are generated by secondary flows through channel bends, a different mechanism from the bed forms.

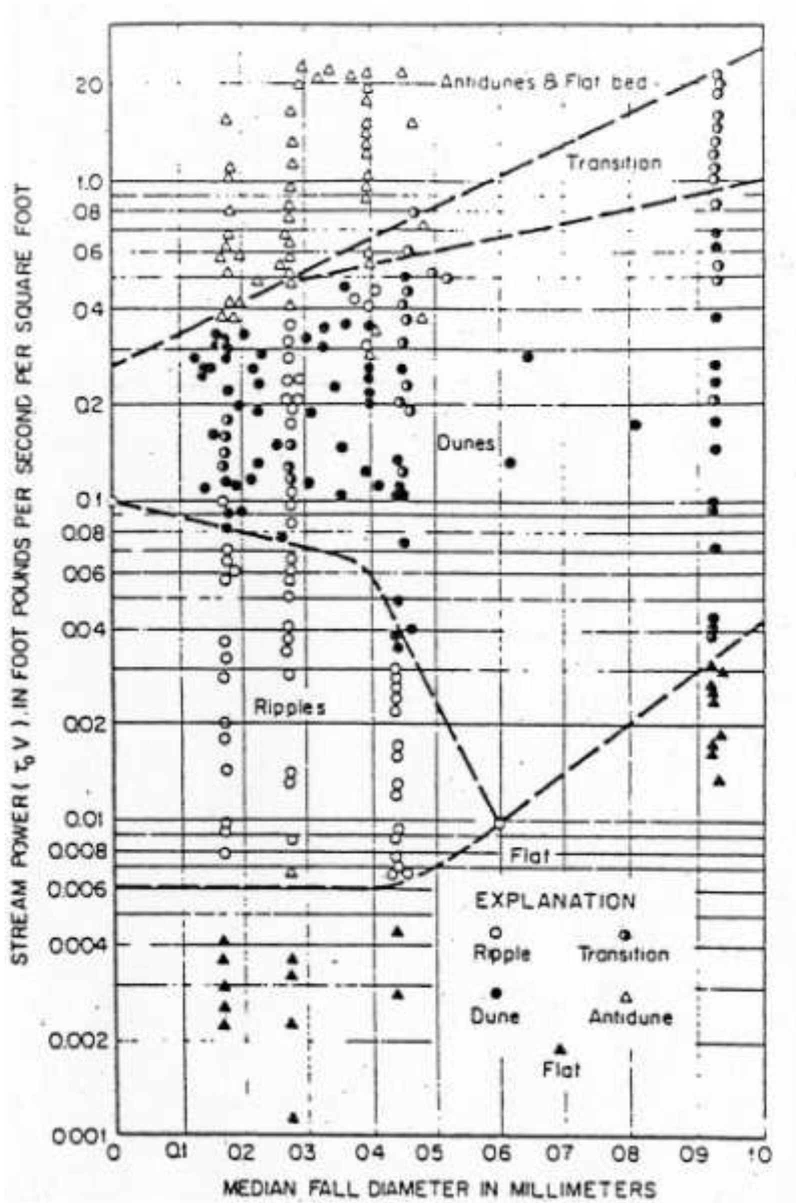

Figure 8-7. Bed Forms as a Function of Stream Power and Fall Diameters of Bed Sediment [Simons and Richardson 1966]

8.4.3 Boundary Shear Stress Calculations

Calculation of the boundary shear stress, τ_0, is required in many alluvial channel computations. Consequently, it is important to know and understand the various methods that are utilized to evaluate boundary shear stress. Equations (7-18) and (7-19) for the boundary shear stress were derived from the basic momentum equation applied to a control volume of uniform flow in a straight channel. For this situation, the distribution of the boundary shear stress across the channel was first described by Lane [1955], as illustrated in Figure 8-8.

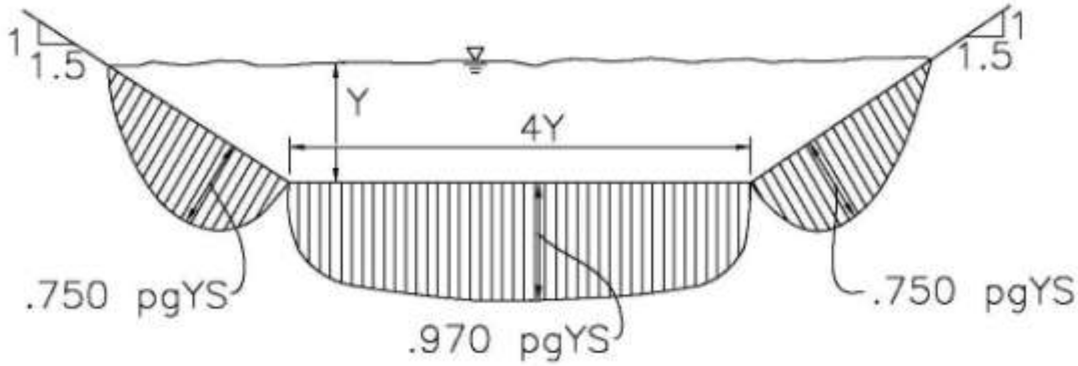

Figure 8-8. Distribution of Boundary Shear Stress

This figure shows an example of the distribution of the boundary shear stress in a trapezoidal channel where the width is 4 times the width. When channel geometries or flows change, as in case of a channel bend, the shear distribution will change. Lane and Carlson [1953] presented the variation in boundary shear stress on channel beds and sidewalls as a function of width-to-depth ratio in Figure 8-9. Note that the boundary shear stress in these curves is divided by ρgYS. For channels of small width/depth ratio (i.e., less than 5), ρgYS will be larger than the mean shear stress ρgRS as calculated by Eq. (7-19). As the width/depth ratio becomes closer to 10, ρgYS approaches ρgRS. Under this condition, as indicated in Figure 8-9, the maximum boundary shear stress and the mean boundary shear stress are equal on the channel bottom, while the maximum value on the side will be about 0.78 times the mean boundary shear stress. For channels of irregular cross-sections, use the depth (Y) defined by hydraulic depth (A/W).

Another issue on shear stress is the separation of shear resistance due to grain roughness from that due to bed form, originally proposed by Meyer-Perter and Muller [1948]. The bed shear stress τ_o is assumed to be made up of two components τ_o' and τ_o'', due to grain roughness and form roughness, respectively. The τ_o' is a tangential stress on the grains lying on the bed, while the τ_o'' is a normal stress on the bed. The relationships are as follows:

$$\tau_o' = \gamma A'S/P = \gamma R'S \qquad (8\text{-}16)$$

and

$$\tau_o'' = \gamma A''S/P = \gamma R''S \qquad (8\text{-}17)$$

whence

$$\tau_o = \tau_o' + \tau_o'' = \gamma RS = \gamma(R' + R'')S \qquad (8\text{-}18)$$

and

$$V_*' = \sqrt{\tau_o' / \rho} = \sqrt{\gamma R' S / \rho} \qquad (8\text{-}19)$$

$$V_*'' = \sqrt{\tau_o'' / \rho} = \sqrt{\gamma R'' S / \rho}$$

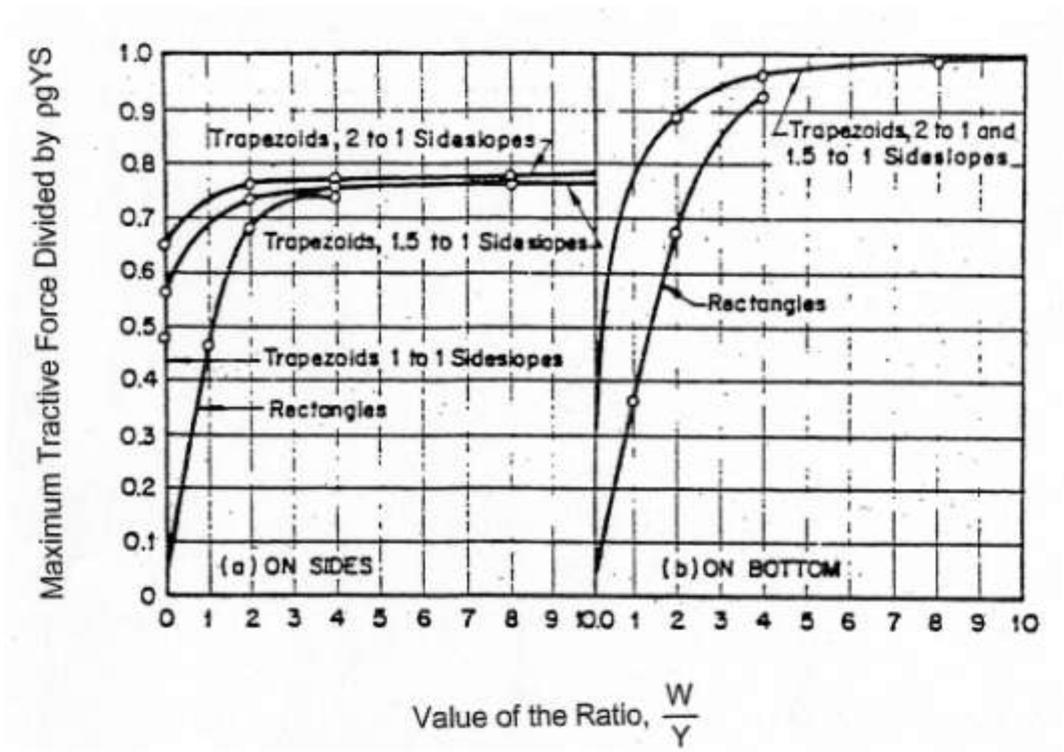

Figure 8-9. Maximum Unit Tractive Force for Various Channel Geometries, Lane and Carlson [1953]

It seems reasonable that Einstein [1950] related the bed load discharge to the tangential stress τ_o', as described in Section 8.2.1, since it is inconceivable that the normal stress is effective in moving sediment at the bed. On the other hand, V_* should be used, instead of V_*', in Eq. (8-2) for computing the suspended load, because the diffusion coefficient for sediment upon which the equation is based depends on the total shear stress.

The above discussion is useful in understanding the mechanisms of sediment transport. We in the Santa Clara Valley are fortunate in the sense that sediments in almost all of our creeks, except the tidal reaches, are coarser than those that are amenable to complex bed forms. Our d_{50} is usually between 5 and 10 mm, compared to the less than 1 mm found in Figure 8-7. Hence, for us, the shear stress due to form roughness, τ_o'', may be ignored in most cases, and the computation is significantly simplified.

For the distribution of shear stress across a channel bend, Figure 8-10 shows the dimensionless boundary shear stress on the outside of a bend as a function of the dimensionless radius of curvature of the bend. For a bend of a radius 5 times that of the channel width, the outside bend is subject to 1.5 times the average shear stress of the cross-section. This figure is excerpted from the US Soil Conservation Services design manual [1977].

8.4.4 Incipient Motion Analysis

The definition of incipient motion is based on the critical or threshold condition where hydrodynamic forces acting on a grain of sediment have reached a value that, if increased even slightly, will move the grain. Under this critical condition or the point of incipient motion, the hydrodynamic forces acting on the grain are just balanced by the resisting forces of the particle.

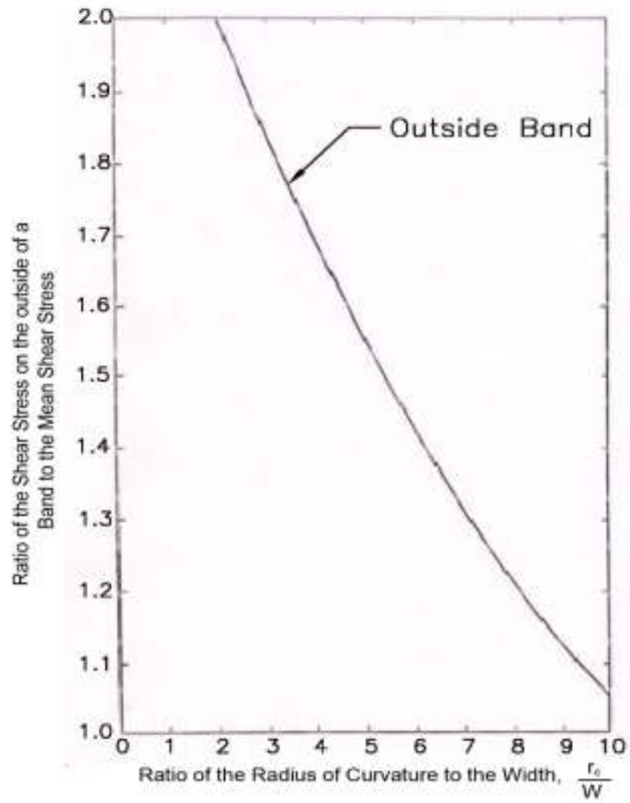

Figure 8-10. Effect of Curvature on Boundary Shear Stress

The concept of incipient motion is of fundamental importance to sediment transport. The Shields diagram (Figures 8-11a and b) may be used to evaluate the particle size at incipient motion for a given discharge, where τ_o is the boundary shear stress, γ_s and γ are the specific weights of sediment and water, d_s is the diameter of the sediment particle size, V_* is the shear velocity, ν is the kinematics viscosity of water.

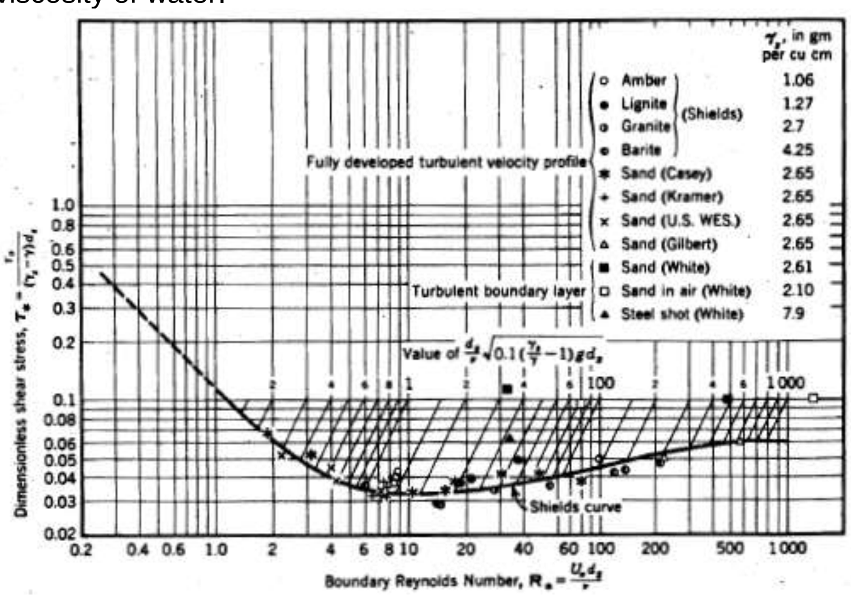

Figure 8-11a. Shields Diagram With Additional Data From Several Other Researchers

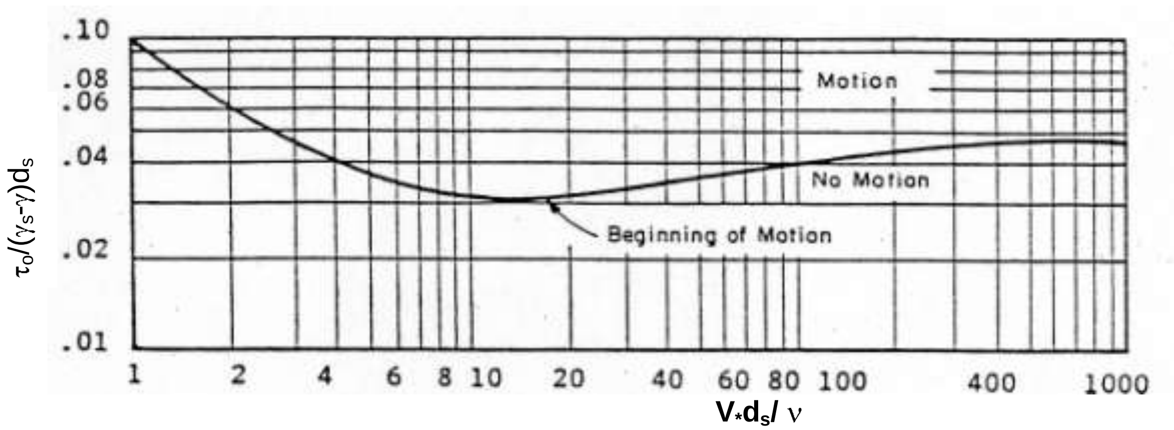

Figure 8-11b. Adjusted Shields Diagram Per Gessler [1971]

The Shield diagram (Figure 8-11a) was developed through measurements of bed load sediment transport for various values of $\tau_o/(\gamma_s - \gamma)d_s$ at least twice as large as the critical value, and then extrapolated to the point of vanishing bed load sediment transport. When the flow is in the turbulent range, about which most hydraulic engineering applications are concerned, Figure 8-11a suggests that the Shields parameter $\tau_o/(\gamma_s - \gamma)d_s$ is independent of flow conditions and approaches a constant value of 0.06. Gessler [1971] re-analyzed the Shields data and found that the bed shear in those experiments included the effect of bed forms. Eliminating the head loss produced by bed forms, and including only the grain shear stress, Gessler [1971] produced Figure 8-11b. Hence, for fully developed turbulent flows, i.e., the pariticle-diameter-Raynolds number higher than 1000, the following relationship exists:

$$d_c = \frac{\tau_o}{0.047(\gamma_s - \gamma)} \tag{8-20}$$

where d_c is the diameter of the sediment particle for conditions of incipient motion, also called the critical diameter, 0.047 is the dimensionless Shields parameter, which was also suggested by Meyer-Peter and Muller [1948]. This equation may be used to estimate critical particle size for non-cohesive sediment. Any consistent set of units may be used.

8.5 SEDIMENT TRANSPORT EQUATIONS

There are numerous sediment transport equations in the literature. Most were developed based on specific sets of data of limited sediment sizes and/or flow conditions. In general, the transport equations are only applicable under the same conditions based on which the equations were calibrated. Beyond those conditions, an equation may be extended, but it would not have been validated. Understanding these limitations is critical to selecting an appropriate transport equation for a particular project. SAM [USACE 2002] developed by the Coastal and Hydraulics Laboratory of the Corps of Engineers provides a comprehensive list of these limiting conditions and comparisons of results when the equations were applied to different flow and sediment environments. Refer to SAM [USACE 2002] for a good understanding of the applicability of these sediment transport equations.

Some equations were developed based on the bed-load transport mechanism alone, and will not be accurate when significant suspended load is expected in the stream. Other equations were developed based on laboratory experiments using well sorted materials, and will not work well when applied directly to graded natural materials. Hence, before selecting a sediment transport method, the bed-material size distribution should first be determined. If necessary for a particular transport method, the sediment distribution curve may be divided into several size fractions. The transport equation is then applied separately to each size fraction. The summation of transport capacities of all size fractions is the total sediment transport capacity. The transport capacity will vary with sediment size, and some loss in accuracy may result from a calculation based on a single representative grain size, such as d_{50} only. The number of size fractions required depends on the accuracy desired and characteristics of the gradation curve. Adequate results are usually obtained using four to six fractions. The mean size of a fraction may be taken as the geometric mean of the upper and lower limiting sizes.

Table 8-2 below summarizes some of the commonly used sediment transport relations and their applications. These equations will be discussed in the following in an abbreviated form focusing on their theoretical basis and applicability, except for the Einstein's bed load and suspend load equations which were discussed in Section 8.2 in more detail and will not be repeated here. Also the focus will be on how these equations may or may not be applied to the environment of the Santa Clara Valley.

Computer programs such as SAM [USACE 2002] will determine size fractions from a gradation curve, select the best-fit transport relationship, calculate the transport capacity for each size-fraction, and calculate the total transport capacity. After one understands the theory behind the transport equations, it is easy to apply these computer programs.

As a final note, it is important to verify computed results against measured data for any transport method. Hence, sampling sediment loads and measuring flow rates during storms is crucial to the success of a sediment transport analysis.

Table 8-2
Summary of Some Commonly Used Sediment Transport Equations

Method	Theoretical Basis				Application	
	Bed Load	**Suspended Load***	**Total Bed-Material Load**	**Total Sediment Load***	**Sand Bed**	**Gravel Bed**
Meyer-Peter & Muller Equation	yes				yes**	yes
Empirical Power Relationships	yes	yes	yes		yes	
Einstein Bed Load Equation	yes				yes	yes
Einstein Suspend Load Methodology		yes			yes	yes
Colby Methodology		yes			yes	
Modified Einstein				yes	yes	yes
Yang's Unit Stream Power Relationships	yes	yes	yes		yes	yes

* Include wash load
** Tend to underestimate sediment discharge. Experience of applying this method to Calabazas Creek (d_{50}=5-10 mm) showed that successful results could be obtained for this type of sand-gravel streams which are common to the Santa Clara Valley.

8.5.1 Meyer-Peter and Muller Equation

Based on experiments with sand particles of uniform sizes, sand particles of mixed sizes, natural gravel, lignite, and baryta, Meyer-Peter and Muller [1948] developed a formula for estimating total bed load transport. Most of the data used in developing this Meyer-Peter & Muller (MPM) equation were obtained in flows with little or no suspended sediment load. A common form of the MPM equation derived for a wide channel with flat bed condition is:

$$q_b = \frac{12.85}{\sqrt{\rho}\,\gamma_s}(\tau_o - \tau_c)^{1.5} \qquad (8\text{-}21)$$

where q_b is the bed load sediment transport rate in cubic feet per second (cfs) per unit width for a specific size of sediment, τ_o is the boundary shear stress, τ_c is the critical shear stress, ρ is the density of water, and γ_s is the specific weight of dry sediment. The critical shear stress is defined by the Shields parameter (Equation 8-20). The boundary shear stress acting under the given flow conditions is defined by Equation 8-18. The mean size of the sediments used in the experiments to develop the MPM relationship ranged from 0.4 mm – 30 mm, and the experimental channel slope varied from 0.04% - 2.0%. If there is significant suspended sediment load, i.e., if the percentage of sand, silt and clay in the bed-material composition is not small, then other methods for calculating suspended bed material sediment transport should be supplemented.

A general form of the MPM equation was presented by Shen [1971] as

$$q_b = k(\tau_o - \tau_c)^m \qquad (8\text{-}22)$$

in which k and m are constants. When the constants in this equation are calibrated with field data, good results are usually attainable, indicating that the approach of using *excess shear stress* as the governing parameter is reasonable for sediment transport.

This method was used successfully to compute sediment transport of the Calabazas Creek between Miller Avenue and Homestead Road. With most of the bed materials in the range of coarse sand to medium gravel, right in the range of the database on which the equation was developed, the MPM method predicted well sediment deposition and degradation patterns.

8.5.2 Empirical Power Relationships

Using a computer generated solution of the Meyer-Peter & Muller bed load sediment transport equation combined with Einstein's integration of the suspended bed material sediment transport, Simons, Li and Fullerton [1981] developed a procedure for estimating the total bed-material load in sand bed channels from power relationships of the following form

$$q_{bmT} = a\,Y_h^b\,V^c \qquad (8\text{-}23)$$

where q_{bmT} is the total bed-material sediment transport rate in cfs per unit width in ft, Y_h is hydraulic depth in ft, V is the average velocity in ft/sec, and a, b, and c are regression coefficients. Using a computer-generated data base, representative values for coefficients a, b, and c were determined for various sediment sizes (d_{50}), gradations (G) and bed slopes. Results of this analysis are presented in Tables 8-3 and 8-4. For evaluation of transport capacity for a sediment size (d_{50}) or gradation coefficient (G) not tabulated, interpolation between the sediment sizes and gradation coefficients bracketing the given size is required. To aid this interpolation, the coefficients from Table 8.3 are plotted in Figures 8-11a, -11b and -11c for bed slopes between 0.001 and 0.01.

Table 8-3

Results of Regression Analysis for Empirical Power Relationships $(q_{bmT} = a\, Y_h^b\, V^c)$ when $0.001 \le S_o \le 0.01$

d_{50}	0.1 mm	0.25 mm	0.5 mm	1.0 mm	2.0 mm	3.0 mm	4.0 mm	5.0 mm
				G =1.0				
a	2.9×10^{-4}	1.81×10^{-5}	3.19×10^{-6}	2.06×10^{-6}	3.45×10^{-6}	5.05×10^{-6}	6.15×10^{-6}	6.35×10^{-6}
b	0.505	0.0446	-0.363	-0.628	-0.693	-0.672	-0.652	-0.639
c	3.43	4.43	5.01	5.03	4.6	4.3	4.13	4.06
				G = 2.0				
a		6.80×10^{-5}	1.48×10^{-5}	3.54×10^{-6}	2.46×10^{-6}	2.81×10^{-6}	3.14×10^{-6}	
b		0.315	0.050	-0.324	-0.587	-0.649	-0.644	
c		3.83	4.31	4.78	4.79	4.62	4.49	
				G = 3.0				
a				5.25×10^{-5}	1.61×10^{-5}	3.71×10^{-6}		
b				0.317	0.112	-0.260		
c				3.76	4.11	4.61		
				G = 4.0				
a				4.31×10^{-5}				
b				0.324				
c				3.7				

S_o = bed slope
q_{bmT} = total bed material sediment transport rate in cfs per unit width (unbulked)
Y_h = hydraulic depth in feet (area / top width)
V = average velocity in ft/sec
G = gradation coefficient = $\frac{1}{2}\left(\frac{d_{84}}{d_{50}} + \frac{d_{50}}{d_{16}}\right)$

Table 8-4

Results of Regression Analysis for Empirical Power Relationships $(q_{bmT} = a\,Y_h^b\,V^c)$ when $0.01 \le S_o \le 0.04$

d_{50}	0.1 mm	0.25 mm	0.5 mm	1.0 mm	2.0 mm	3.0 mm	4.0 mm	5.0 mm
				G =1.0				
a	$4.74x10^{-4}$	$7.45x10^{-5}$	$1.66x10^{-5}$	$5.80x10^{-6}$	$3.58x10^{-6}$	$3.62x10^{-6}$	$4.03x10^{-6}$	$4.50x10^{-6}$
b	0.557	0.305	0.0530	-0.198	-0.427	-0.532	-0.587	-0.615
c	3.22	3.76	4.17	4.42	4.45	4.37	4.27	4.18
				G = 2.0				
a		$1.27x10^{-4}$	$3.81x10^{-5}$	$1.16x10^{-5}$	$5.25x10^{-6}$	$4.20x10^{-6}$	$3.89x10^{-6}$	
b		0.383	0.199	-0.0318	-0.264	-0.385	-0.459	
c		3.56	3.88	4.18	4.33	4.34	4.31	
				G = 3.0				
a			$7.40x10^{-5}$	$3.02x10^{-5}$	$1.08x10^{-5}$			
b			0.310	0.161	-0.0502			
c			3.65	3.86	4.10			
				G = 4.0				
a				$5.30x10^{-5}$				
b				0.264				
c				3.67				

S_o = bed slope

q_{bmT} = total bed material sediment transport rate in cfs per unit width (unbulked)

Y_h = hydraulic depth in feet (area / top width)

V = average velocity in ft/sec

G = gradation coefficient = $\frac{1}{2}\left(\frac{d_{84}}{d_{50}} + \frac{d_{50}}{d_{16}}\right)$

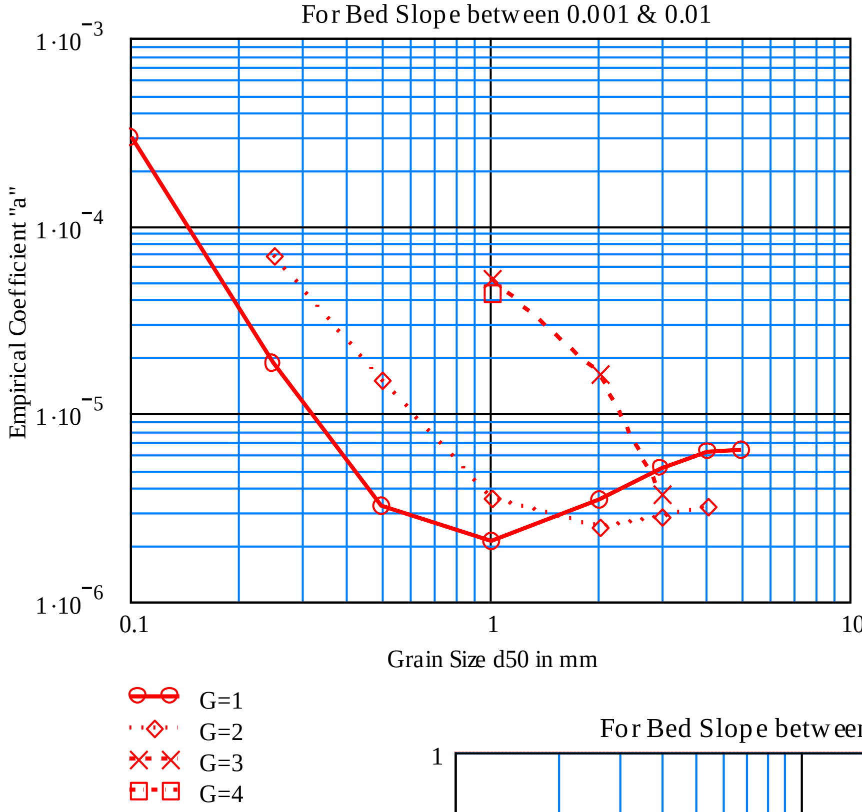

Figure 8-11a. Empirical Coefficient "a" of the Simmons, Li & Fullerton Power Relationship

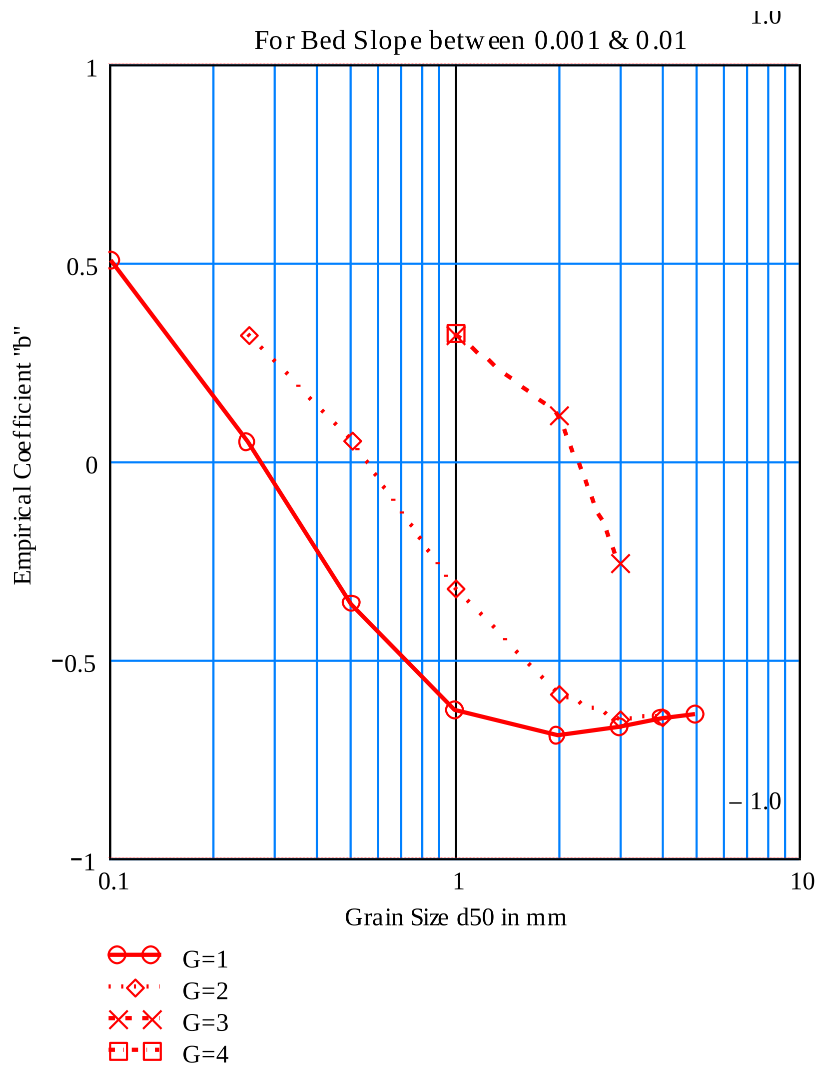

Figure 8-11b. Empirical Coefficient "b" of the Simmons, Li & Fullerton Power Relationship

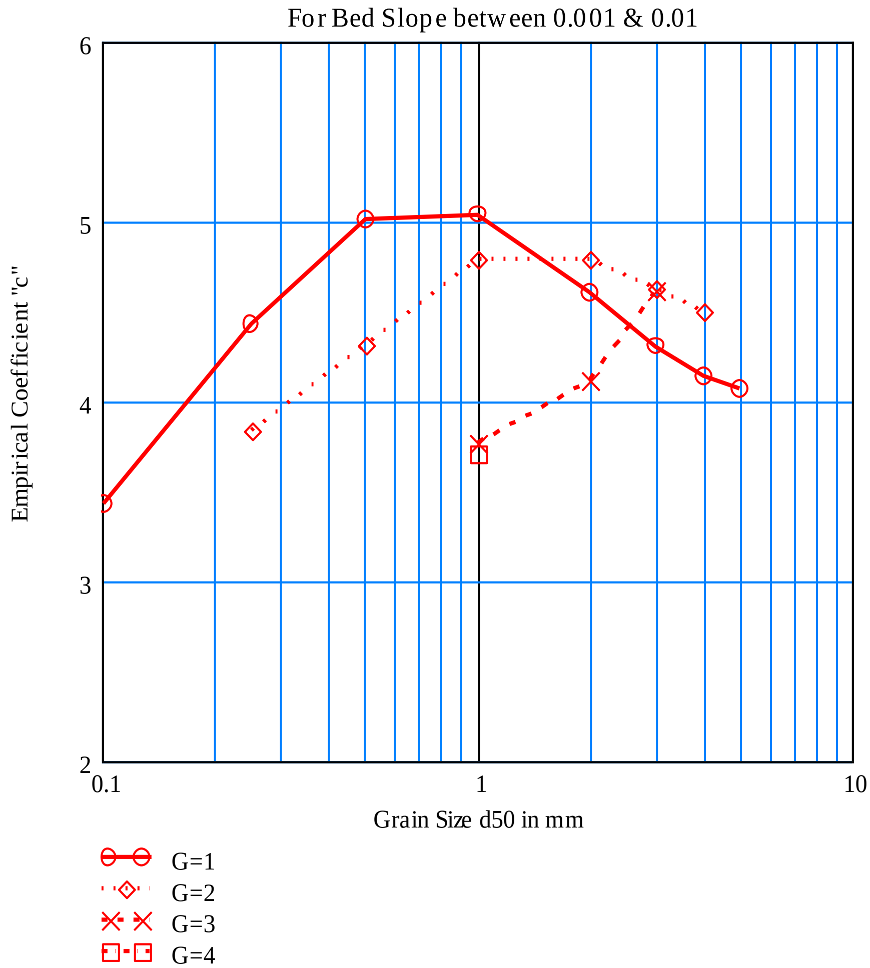

Figure 8-11c. Empirical Coefficient "c" of the Simmons, Li & Fullerton Power Relationship

The values of b and c indicate that sediment transport rates are more dependent on velocity than depth. Sediment transport for the finer sediment sizes is directly proportional to depth, as reflected by the positive b values, whereas transport of coarser sizes is inversely proportional to depth, as b becomes negative. This is because the smaller material is more easily suspended and the resulting suspended sediment concentrations are more uniform. Thus, for a given velocity the larger the depth, the greater the amount of sediment will be suspended. Larger sediment particles, on the other hand, are more difficult to suspend and keep in suspension. For a given velocity, as depth increases the intensity of turbulent transfer properties and the bottom shear stress decrease, resulting in an inverse relationship between transport and depth for larger particles.

As an alternative to Equation 8-23 and Tables 8-3 and 8-4, a single relationship was developed by Zeller and Fullerton [1983]:

$$q_{bmT} = 0.0064 \frac{n^{1.77} V^{4.32} G^{0.45}}{Y_h^{0.30} d_{50}^{0.61}} \tag{8-24}$$

where n is Manning's roughness coefficient, V is the mean velocity, G is the gradation coefficient (see Table 8-3), Y_h is the hydraulic depth, and d_{50} is the median bed-material particle diameter. In this equation all units are in ft-lb-sec system, except d_{50}, which is in millimeters.

Table 8-5 lists the range of parameters considered in the development of the relations given in Tables 8-3 and 8-4 and Equation 8-24**.** Since the equations were developed for sand bed alluvial channels, they do not apply to conditions where the bed/bank material has cohesive properties. Transport rates will be over-predicted for cohesive channel conditions. For conditions meeting the criteria of Table 8-5, Equation 8-23 or 8-24 should provide results within ten percent of the theoretical values computed with the Meyer-Peter & Muller bed load and Einstein suspended bed-material load methodologies that were used to develop the regression equations.

Table 8-5
Range of Parameters Examined for Power Relationship

	Value Range	
Parameter	**Equation 8-23 when used with Tables 8-3 and 8-4**	**Equation 8-24**
Froude Number	< 4	Unlimited
Velocity	5 – 26 (ft/s)	3 – 30 (ft/s)
Manning's n	0.025	0.018 – 0.035
Bed Slope	0.001 – 0.040	0.001 – 0.04
Unit Discharge	5 – 200 (cfs/ft)	10 – 200 (cfs/ft)
Particle Size	$D_5 \geq 0.062$ mm $D_{90} \leq 15$ mm	0.5 mm $\leq D_{50} \leq$ 10 mm
Depth	Unlimited	1 – 20 ft
Armoring	No	No
Gradation Coefficient	1 - 4	2 - 5

Although most of the ranges of parameters listed above fall into the conditions of the Santa Clara Valley, the applicability of this method is still limited for two reasons. Firstly, the actual data used to calibrate the method came mostly from the southwestern states such as Arizona and Texas. Gradation of the sand-bed materials found in those states is quite different from the Bay Area. That is why the regression and gradation coefficients in Tables 8-3 and 8-4 do not cover our creek data adequately. Secondly, we have armoring in a lot of our creek reaches, which does not exist in the alluvial rivers in the Southwest.

8.5.3 Colby's Approach

Colby [1964] developed the graphical procedure shown in Figures 8-12 to 8-15 for determining bed material sediment transport rate in sand bed alluvial channels as a function of average flow velocity. In developing his computational curves, Colby was guided by Einstein's bed load function (Equations 8-8 and 8-9 and Figures 8-6a, -6b & -6c) and an immense amount of data from streams and flumes. However, it should be understood that in Figure 8-12 all curves for the 100 ft depth, most curves of the 10 ft depth, and some of the curves of 1 ft and 0.1 ft depth were not based entirely on measured data, but were developed from limited data and theory. The curves represent six median sand-particle sizes (0.1, 0.2, 0.3, 0.4, 0.6 and 0.8 mm) at water temperature of 60^{o}F.

The applicability of Colby's method to streams in the Santa Clara Valley is limited by the fact that few of our creek reaches has a d_{50} between 0.1 and 1 mm.

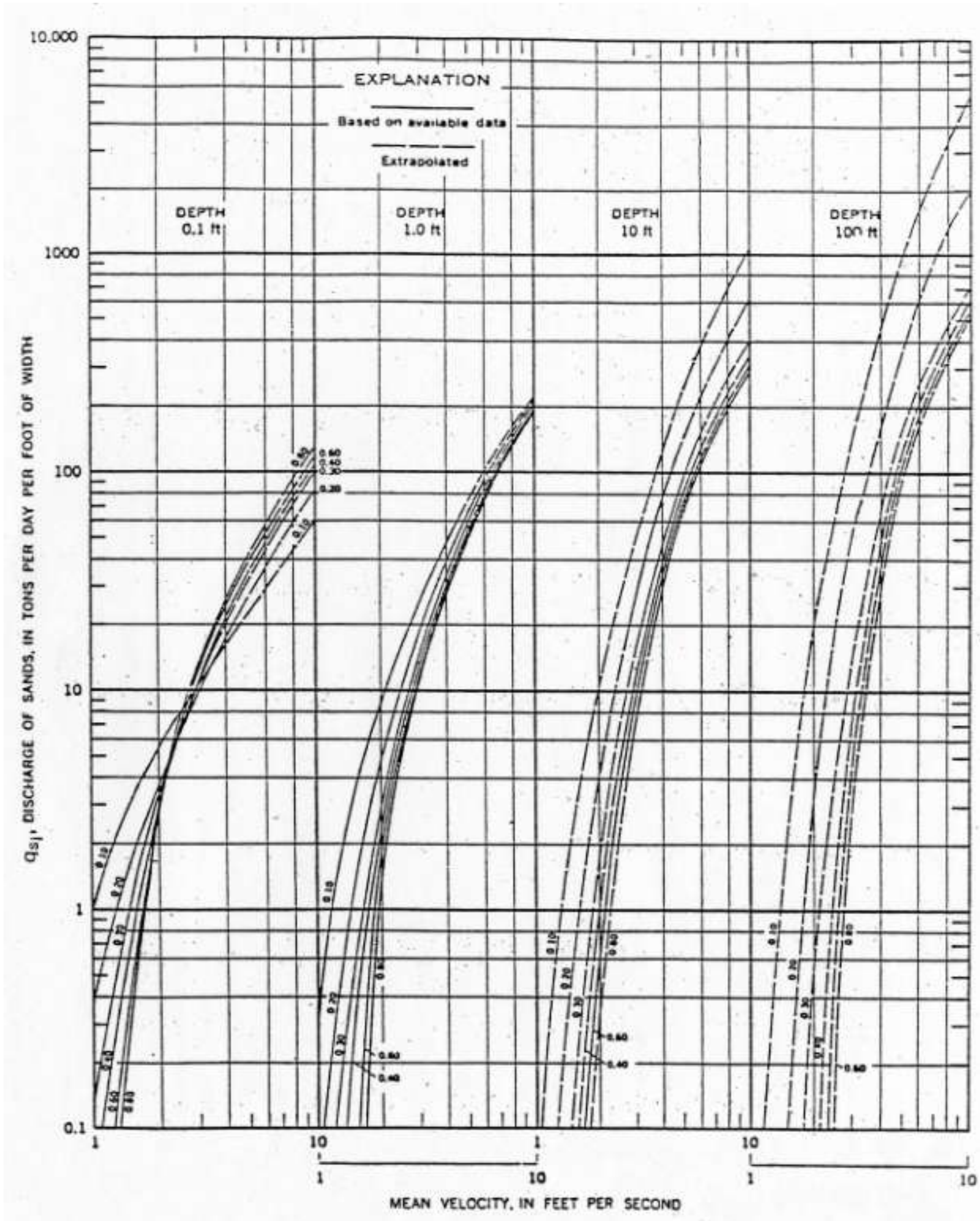

Figure 8-12. Colby [1964] Bed Load Transport Relationships

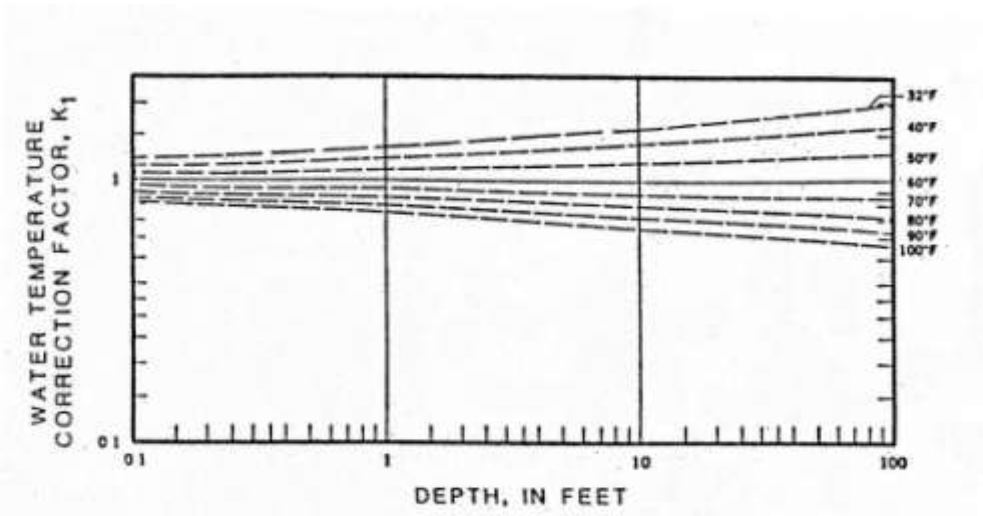

Figure 8-13. Water Temperature Correction Factor

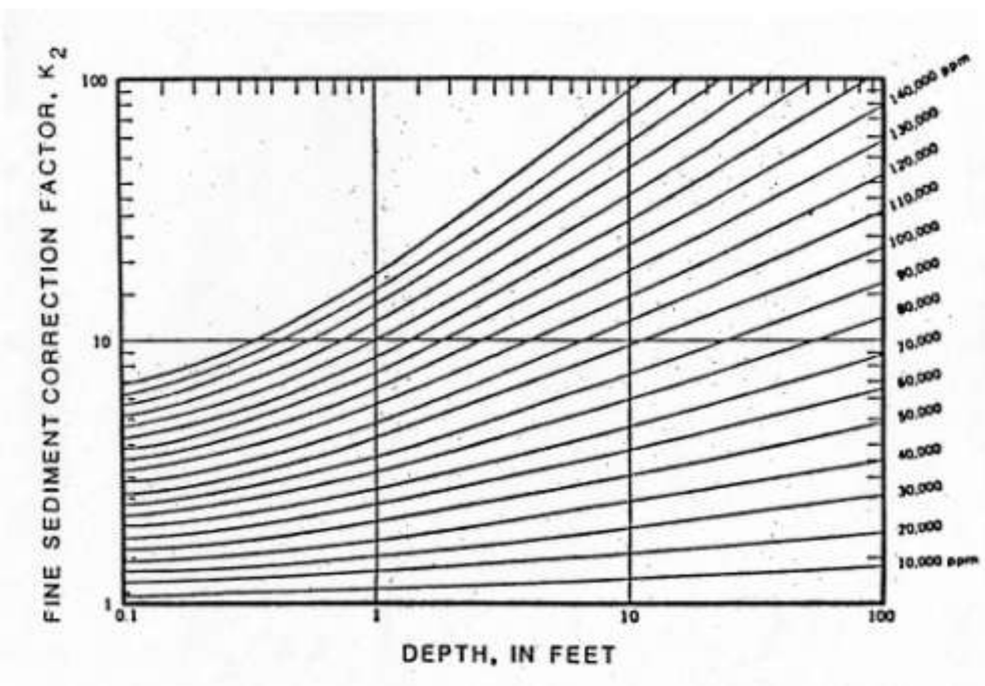

Figure 8-14. Fine Sediment Correction Factor

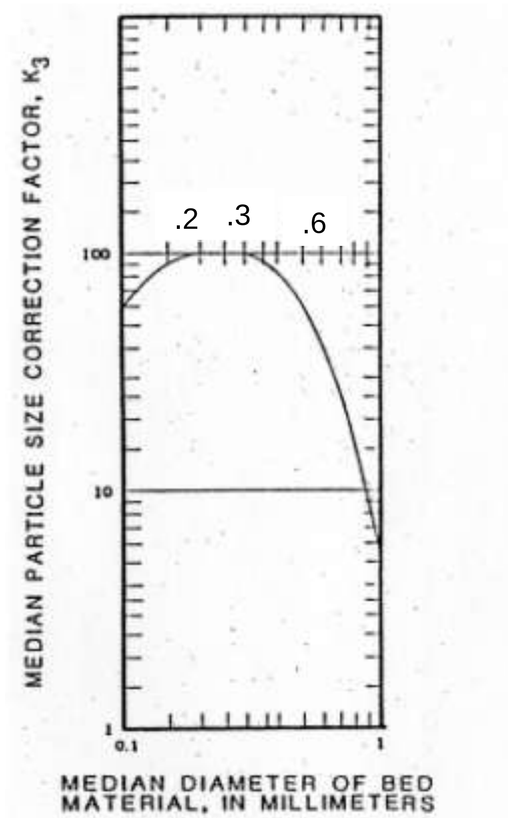

Figure 8-15. Correction for Median Particle Size

In utilizing Figures 8-12 to 8-15 to compute the bed-material sediment transport rate, the following procedure is required:

1. The required data are mean velocity V, depth (typically hydraulic depth), $Y_{h,}$ median size of bed material d_{50}; water temperature; and fine sediment (silt and clay) concentration.
2. The uncorrected sediment discharge q_{si} for the given V, Y_h, and d_{50} can be obtained from Figure 8-12 for the two depths that bracket the desired depth. Interpolate on a logarithmic graph of depth vs. q_{si} to determine the desired q_{si} for the actual depth.
3. Two correction factors, k_1 and k_2, shown in Figure 8-13 and 8-14 respectively, account for the effect of water temperature and fine suspended sediment on the bed-material transport rate. If the bed-material size falls outside the 0.2 mm to 0.3 mm range, factor k_3 from Figure 8-15 is applied to correct for sediment size effect.
4. The total bed material sediment transport rate q_{bmT} with the corrections of temperature effect, presence of fine suspended sediment, and sediment size is given by

$$q_{bmT} = [1 + (k_1 k_2 - 1) 0.01 k_3]\, q_{si} \tag{8-25}$$

Figure 8-13 shows that $k_1 = 1$ when the temperature is 60^oF. Figure 8-14 shows that $k_2 = 1$ when the concentration of fine sediment is negligible. And Figure 8-15 shows that $k_3 = 1$ when d_{50} lies between 0.2 mm to 0.3 mm.

8.5.4 Modified Einstein Method

The modified Einstein method was developed by Colby and Hembree [1955] to estimate the total bed-material discharge once suspended and bed loads and bed-material samples as well as flow data are collected. The required data include flow discharge Q, mean velocity V, cross-sectional area A, stream width W, average depth Y, size distribution of the measured suspended sediment load, and size distribution of the bed-material.

It is simply a method to separate the wash load from the measured sediment discharge and use the resulting bed-material load in Einstein's bed load and suspended load formulae to develop an equation for sediment discharge. The difference between this method and the Einstein method is that here the measured data are used to back-calculate z (in Equation 8-6) while the Einstein method used an empirical equation [Rubey, 1933] to calculate fall velocity and z.

The details of this method will not be given here. A user may refer to pp. 214-217 of ASCE [1975] for details. It suffices to note that the z defined by the modified, as well as the original, Einstein method contains V_*', the shear velocity due to grain roughness, while the z defined by the Rouse suspension theory (Eq. 8-2) contains V_*, the total shear velocity. For the creeks in our jurisdiction, this difference is negligible. As a side note, the z computed by the modified Einstein method is proportional to the 0.7^{th} power of the fall velocity, while the z used in the original Einstein method is proportional to the fall velocity.

8.5.5 Unit Stream Power Method

Bagnold [1966] introduced the concept of stream power to the study of sediment transport. He defined stream power as the product of shear stress along the bed and the average flow velocity. Thus, the stream power has the dimension of power per unit bed area. Bagnold used this concept to develop a bedload transport equation and later extended it to cover suspended load and total load. Engelund and Hansen [1967] and Ackers and White [1983] also used the same concept to develop their respective transport equation.

Yang [1972] used the same approach and hypothesized that the rate of sediment transport, i.e., sediment concentration, should be related to the rate of energy dissipation of the stream, i.e., stream power. He defined unit stream power as the product of average flow velocity and energy slope. Thus this unit stream power has the dimension of power per unit weight of water. Using experimental data, and a dimensional analysis to convert stream power into dimensionless parameters that include sediment size, particle fall velocity, shear velocity, average flow velocity and energy slope, Yang developed a dimensionless stream power equation for sand and one for gravel. The equation for sand is shown as Eq. (8-26):

$$\log C_{ts} = 5.435 - 0.286\log\frac{wd}{v} - 0.457\log\frac{V_*}{w} + (1.799 - 0.409\log\frac{wd}{v} - 0.314\log\frac{V_*}{w})\log(\frac{VS}{w} - \frac{V_{cr}S}{w}) \quad (8\text{-}26)$$

where C_{ts} = total sand concentration in parts per million by weight

w = particle fall velocity

d = mean sediment size in mm

v = kinematic viscosity of water

V_* = shear velocity

V = average flow velocity
S = energy slope
V_{cr} = critical flow velocity at incipient of motion

The equation for gravel is shown as Eq. (8-27):

$$\log C_{tg} = 6.681 - 0.633\log\frac{wd}{v} - 4.816\log\frac{V_*}{w} + (2.784 - 0.305\log\frac{wd}{v} - 0.282\log\frac{V_*}{w})\log(\frac{VS}{w} - \frac{V_{cr}S}{w}) \quad (8\text{-}27)$$

where C_{tg} = total gravel concentration in parts per million by weight.

The total sediment in a stream may be divided into several size fractions for sand and gravel, use the above equations to compute the concentration in each size fraction (C_i), and sum up for the total bed material concentration (C_t) using the relationship:

$$c_t = \sum_{i=1}^{n} p_i c_i$$

where p_i is the percent by weight of the material in the i^{th} size fraction.

The above discussion on sediment transport equations is by no means complete. There are many more equations in SAM [USACE 2002], HEC-6 [USACE 1993], HEC-6T [MBH 2002], and the new version 4 of HEC-RAS [USACE 2006] that are not mentioned here. The objective has been to describe the physical mechanism of sediment transport and the engineering treatment of this physical phenomenon. With this understanding of the underlying physics, one can determine how an appropriate transport equation may be selected, calibrated and applied to a real reach of our creeks, as will be discussed further in Chapter 2.

BIBLIOGRAPHY

Ackers, P. and W. R. White, “Sediment Transport: New Approach and Analysis,” *Journal of Hydraulic Division*, ASCE, Vol. 99, No. HY11, November 1973, pp. 2041-2060.

ASCE (American Society of Civil Engineers), *Sedimentation Engineering*, ASCE Manuals and Reports on Engineering Practice – No. 54, 1975.

Anderson, A.G., et al., “Tentative Design Procedure of Riprap Lined Channels,” *Project Report No. 96*, St. Anthony Falls Hydraulic Lab., Minneapolis, Minnesota, NCHRP, Rep.108, 1970.

Bagnold, R. A., “An Approach to the Sediment Transport Problem From General Physics,” U.S. Geological Survey Professional Paper 422-I, 1966.

Bathurst, J. C., “Flow Resistance of Large-Scale Roughness,” *Journal of the Hydraulics Division*, ASCE, Vol. 104, No. HY12, Proc. Paper 14239, pp. 1587-1603, 1978.

Brown, C. B., “Sediment Transportation,” Chapter XII, *Engineering Hydraulics*, H. Rouse, ed., John Wiley and Sons, Inc., New York, N.Y., 1950.

Brownlie, W. R., “Flow Depth in Sand-Bed Channels,” *Journal of Hydraulic Division*, ASCE, Vol. 109, No. 7, July 1983, pp. 959-990.

Chow, V. T., *Open-Channel Hydraulics*, McGraw-Hill, New York, 1959.

Colby, B. R., “Practical Computations of Bed-Material Discharge,” *Journal of the Hydraulics Division*, ASCE, Vol. 90, No. HY2, 1964.

Colby, B. R., and C. H. Hembree, “Computation of Total Sediment Discharge, Niobrara River near Cody, Nebraska,” U.S. Geological Survey Water Supply Paper 1357, 1955.

Einstein, H. A., “The Bed Load Function for Sediment Transportation in Open Channel Flows,” U.S. Department of Agriculture, Soil Conservation Service, Technical Bulletin No. 1026, 1950.

Einstein, H. A. and Barbarossa, N., “River Channel Roughness,” *Transactions*, ASCE, Vol. 117, Paper No. 2528, pp. 1121-1146, 1952.

Gessler, J., 1971. “Beginning and Ceasing of Sediment Motion,” *River Mechanics*, Chapter 7, edited by H. W. Shen, Fort Collins, Colorado, 22 pp, 1971.

Keulegan, G. H., “Laws of Turbulent Flows in Open Channels,” *J., National Bureau of Standards*, Vol.21, Research Paper 1151, pp 707-741,1938.

Lane, E. W., “The Importance of Fluvial Morphology in Hydraulic Engineering,” *Proceedings* ASCE, Vol. 81, No. 745, pp. 1-17, 1955.

Lane, E. W. and E. J. Carlson, “Some Factors Affecting the Stability of Canals Constructed in Coarse Granular Materials,” *Proceedings,* Minnesota International Hydraulics Convention, September 1953.

Laursen, E. M., “The Total Sediment Load of Streams,” *Journal of the Hydraulic Division*, ASCE, Vol. 54, No. HY1, Proceeding Paper 1530, Feb., 1958, pp. 1-36.

Maynord, S. T., “Flow Resistance of Riprap,” *Journal of Hydraulic Engineering*, ASCE, Vol. 117, No. 6, 1991, pp. 687-693.

MBH, Sedimentation in Stream Networks (HEC-6T), *User Manual*, MBH Software, Inc., January 2002.

Meyer-Peter, E., and R. Muller, “Formulas for Bed Load Transport,” *Proceedings,* 3rd Meeting of IAHR, Stockholm, pp. 39-64, 1948.

Philip Williams & Associates, Ltd., “Sediment Transport Modeling Study of the Upper Guadalupe River, Phase 2,” Report prepared for the San Francisco District Corps of Engineers, January 1996

Rouse, H., “Modern Conceptions of the Mechanics of Fluid Turbulence,” *Transactions*, ASCE, Vol. 102, Paper No. 1965, 1937, pp. 463-543.

Rubey, W. W., “Settling Velocities of Gravel, Sand and Silt Particles,” *American Journal of Science*, 5th series, Vol. 25, No. 148, 1933, pp. 325-338.

Shields, I. A., “Application of Similarity Principles and Turbulence Research to Bed-Load Movement,” A translation from the German by Ott W. P. and J. C. van Vchelin, U. S. Soil Conservation Service Coop. Lab., California Inst. of Tech., Pasadena, California, 1936.

Simons, D. B., R. M. Li and W. T. Fullerton, “Theoretically Derived Sediment Transport Equations for Pima County, Arizona,” Simons, Li & Associates, Inc., Fort Collins, Colorado, *Report,* prepared for Pima County DOT and Flood Control District, Tucson, Arizona, 1981.

Simons, D. B., and E. V. Richardson, “Resistance to Flow in Alluvial Channels,” U.S. Geological Survey Professional Paper 422-J, 1966.

Simons, D. B., and F. Senturk, Sediment Transport Technology, Water Resources Publications, Fort Collins, Colorado, 1977.

Simons, Li & Associates, Inc., *Engineering Analysis of Fluvial Systems*, published by Simons, Li & Associates, printed and bound by Book Crafters, Inc., Chelsea, Michigan, 1982.

Strickler, A., “Some Contributions to the Problem of the Velocity Formula and Roughness Factors for Rivers, Canals, and Closed Conduits,” *Mitteilungen des eidgenossischen Amtes fur Wasserwirtschaft*, Bern, Switzerland, No. 16, 1923

Toffaletti, F. B., “Definitive Computations of Sand Discharge in Rivers,” *Journal of the Hydraulics Division*, ASCE, Vol. 95, No. HY1, Proceeding Paper 6350, Jan., 1969, pp. 225-248.

U.S. Army Corps of Engineers, “HEC-RAS River Analysis Systems,” *User’s Manual*, Version 4.0 Beta, CPD-68, Hydrologic Engineering Center, November 2006.

U.S. Army Corps of Engineers, “Berryessa Creek Project General Reevaluation Study and Report,” *Technical Appendices*, February 2004.

U.S. Army Corps of Engineers, “SAM Hydraulic Design Package for Channels,” Final Report, prepared by William A. Thomas, Ronald R. Copeland and Dinah N. McComas, Coastal and Hydraulics Laboratory, Engineering Research and Development Center, Vicksburg, MS, 2002.

U.S. Army Corps of Engineers, “Scour and Deposition in Rivers and Reservoirs,” *User’s Manual*, Hydrologic Engineering Center (HEC), 1993.

U.S. Soil Conservation Services, Design of Open Channels, Engineering Division, Technical Release No. 25, Washington, D.C., 1977.

Yang, C. T., “Unit Stream Power Equation for Gravel,” *Journal of Hydraulic Division*, ASCE, Vol. 110, No. 12, December 1984, pp. 1783-1797.

Zeller, M. E., and W. T. Fullerton, “A Theoretically Derived Sediment Transport Equation for Sand-Bed Channels in Arid Regions,” *Proceedings* of the D. B. Simons Symposium on Erosion and Sedimentation, R. M. Li and P. F. Lagasse (eds.), 1983.